

THE ASTROPHYSICAL JOURNAL

AN INTERNATIONAL REVIEW OF SPECTROSCOPY AND
ASTRONOMICAL PHYSICS

VOLUME 85

MARCH 1937

NUMBER 2

ROWLAND GHOSTS

HENRY G. GALE

ABSTRACT

A number of small diffraction gratings have been ruled containing arbitrary errors. It is shown that a small sine error $a_i \sin \theta$ produces ghosts the intensity of which depends upon the ratio of a_i to a_0 , the average grating space, and the order N , in complete agreement with Rowland's theory. Small periodic errors may be applied simultaneously, and each will produce a ghost corresponding to its period. When the errors are small, the ghosts appear at the expected places, and the shape of the error curve may be interpreted from the positions and strength of the ghosts.

The new ruling engine at the Ryerson Physical Laboratory has been described briefly, and some mention made of its performance, in the *Journal of Scientific Instruments*, **12**, 32, 1935, in the *Zeeman Verhandelingen*, p. 280, The Hague, 1935, and in *Science*, **85**, 25, 1937.

Papers have been read before the joint meeting of the American Physical Society and Section B of the American Association for the Advancement of Science at the St. Louis meeting, December, 1935; at the joint meeting of the American Physical Society and the Optical Society of America, in New York, February, 1936; and at the Chicago meeting of the National Academy of Science, November, 1936.

The interest shown by spectroscopists in the results on Rowland ghosts seems to call for further publication.

A grating ruled with uniform spacing, a_0 , will give in any order

N , a single sharp image of any monochromatic spectrum line of wave-length λ , in accordance with the relation,

$$a_0 (\sin i + \sin \theta) = N\lambda,$$

where i is the angle of incidence and θ the angle of diffraction. If $\lambda = 2\pi/b$, we have

$$\mu = \frac{2\pi N}{ba_0} = \sin i + \sin \theta.$$

If periodic errors are present in the ruling, false lines, or "ghosts," appear. The theory defining their position and intensity has been given by Rowland.¹ If simple sine errors occur for each group of m lines, the distance y of the r^{th} ruling from one end of the grating will be given by

$$y = a_0 r + a_1 \sin e_1 r + a_2 \sin e_2 r + \dots,$$

where $e_k = 2\pi/m_k$ and a_k is the maximum displacement of any ruling from the correct position, owing to the error e_k .

In the simple case where all values of a_k are zero except a_0 and a_1 , Rowland's theory gives the position of the spectrum line and its ghosts as shown in Table 1.

$J_n(u)$ is a Bessel function of u of order n and is determined by the following equation:

$$J_n(u) = \frac{u^n}{2^n n!} \left(1 - \frac{u^2}{2^2(n+1)} + \frac{u^4}{2^4 2! (n+1)(n+2)} - \frac{u^6}{2^6 3! (n+1)(n+2)(n+3)} + \dots \right).$$

Since here $u = b\mu_p a_1 = (2\pi[N + (p/m)] a_1/a_0)$, when m is large, usually several hundred in the case of the Rowland ghosts, $b\mu_p a_1$ does not differ from $b\mu a_1$ by more than about 1 per cent, and the values of $J_n^2(b\mu_p a_1)$ will differ from the values of $J_n^2(b\mu a_1)$ by much less than 1 per cent, as is shown by the curves of Figure 1, which are graphs of $J_0^2(u)$, $J_1^2(u)$, $J_2^2(u)$, and $J_3^2(u)$. It is therefore sufficiently accurate to

¹ *Phil. Mag.*, **35** (5), 397, 1893; *Astronomy and Astrophysics*, **12**, 129, 1893; Rowland's *Physical Papers*, p. 525.

use $u = 2\pi N(a_1/a_0)$ instead of $u = (2\pi[N + (p/m)] a_1/a_0)$ in calculating the intensities of the ghosts. Table 2 gives the values of $J_n^2(u)$ for different values of n and of $u = 2\pi N(a_1/a_0)$.

TABLE 1

Position	Intensity	Description
$\mu = \frac{2\pi N}{ba_0}$	$J_0^2(b\mu a_1)$	Principal line
$\mu_1 = r \pm \frac{e_1}{ba_0}$	$J_1^2(b\mu_1 a_1)$	First ghost
$\mu_2 = r \pm \frac{2e_1}{ba_0}$	$J_2^2(b\mu_2 a_1)$	Second ghost
$\mu_3 = r \pm \frac{3e_1}{ba_0}$	$J_3^2(b\mu_3 a_1)$	Third ghost
.....

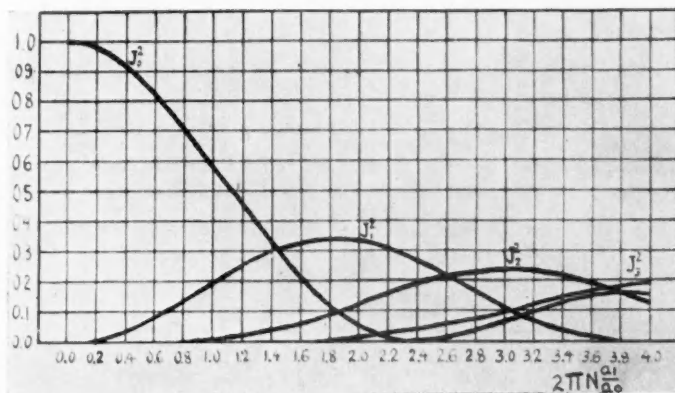


FIG. 1

When $a_1 = 0$, the case of no periodic error, $J_0^2(u)$ has its maximum value and all the other J 's are equal to 0; the main line has its maximum value and there are no ghosts. As a_1 is increased, u increases and J_0 decreases. The other functions J_n begin to have finite values, and the ghosts appear.

Table 2 and the curves show that the principal line itself will be

reduced to 0 in intensity when $2\pi Na_1/a_0 = 2.405$. This will occur in the third order, $N = 3$, when $a_1/a_0 = 0.1274$, i.e., when the maximum displacement, a_1 , in each period is about one-eighth of the grating space, a_0 , when there are 600 rulings per millimeter. The distance, a_1 , is most conveniently measured by an interferometer, the back mirror of which is mounted on the grating carriage. When

TABLE 2

$2\pi Na_1/a_0$	J_0^2	J_1^2	J_2^2	J_3^2	J_4^2	J_5^2	J_6^2	J_7^2
0.0	1.000							
0.2	0.980	0.010						
0.4	0.922	.038	0.000					
0.6	0.832	.082	.002					
0.8	0.716	.136	.005					
1.0	0.586	.194	.013	0.000				
1.2	0.450	.248	.025	.001				
1.4	0.321	.294	.043	.003				
1.6	0.207	.325	.066	.006				
1.8	0.116	.338	.094	.010	0.001			
2.0	0.050	.333	.124	.017	.001			
2.2	0.012	.309	.157	.027	.002			
2.405	0.000	.269	.186	.040	.003			
2.6	0.009	.222	.212	.055	.007	0.001		
2.8	0.034	.168	.228	.075	.011	.001		
3.0	0.068	.115	.236	.096	.017	.002		
3.25	0.111	.058	.231	.123	.028	.005		
3.5	0.144	.019	.210	.150	.042	.006	0.001	
3.75	0.161	.001	.176	.171	.059	.011	.001	
3.832	0.162	.000	.162	.176	.065	.013	.002	
4.0	0.158	.004	.133	.185	.079	.017	.002	
4.25	0.136	.020	.088	.188	.100	.026	.004	0.000
4.5	0.103	.053	.047	.180	.121	.038	.007	.001
4.75	0.065	.084	.018	.161	.140	.052	.011	.002
5.0	0.031	0.107	0.002	0.133	0.153	0.068	0.017	0.003

$\lambda 5460$ is used, $a_0 = 1/600$ mm = 6.1 fringes; and when $a_1/a_0 = 0.1274$, a_1 is about three-quarters of a fringe. For this value of a_1 , the first ghosts (one on each side), given by $J_1^2(u)$, have already passed their maximum intensities and are 26.9 per cent as strong as the original line. The second ghosts, given by $J_2^2(u)$, have an intensity 16.6 per cent; the third ghosts, given by $J_3^2(u)$, are 4 per cent; $J_4^2(u)$ equals 0.3 per cent; and higher ghosts are too faint to consider. Further, since we know that $1 = J_0^2 + 2J_1^2 + 2J_2^2 + \dots$, we should expect the sum of all the intensities to be 1; and we have,

from the curves, $2 \times 26.9 + 2 \times 18.6 + 2 \times 4.0 + 2 \times 0.3 = 99.6$, when the intensity of the central line without ghosts is taken as unity. The small residual, 0.4 per cent, is distributed among ghosts of higher order. Table 2 shows further that when

$$u = \frac{2\pi N a_1}{a_0} = 3.832, \text{ i.e., } \frac{a_1}{a_0} = 0.203,$$

$J_1^2(u)$ is 0 and the first ghost disappears. The main line is 16.2 per cent, the second ghost 16.2 per cent, the third ghost 17.6 per cent,

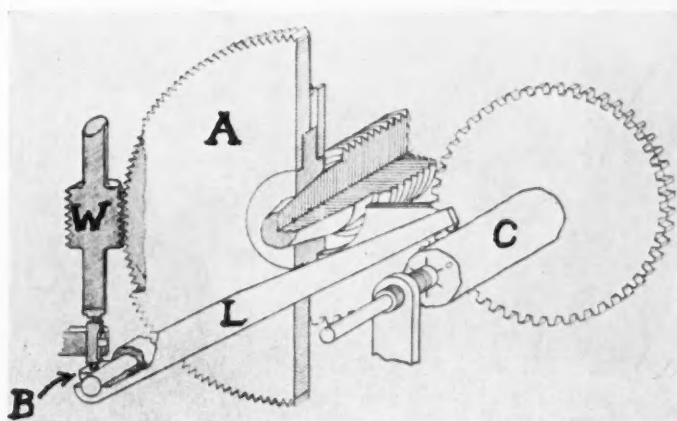


FIG. 2

the fourth ghost 6.5 per cent, the fifth ghost 1.3 per cent, and the sixth ghost 0.2 per cent. The sum is 100 per cent, since here again $16.2 + 2 \times 16.2 + 2 \times 17.4 + 2 \times 6.5 + 2 \times 0.4 = 100$.

The ruling engine at the Ryerson Physical Laboratory is provided with a compensating cylinder, C , Figure 2, which carries the long end of the lever, L . The short end of the lever carries the end butt, B , of the worm, W , which drives the worm wheel, A . A motion of 3.50 mm at C produces a motion of one fringe at the ruling carriage.

The cylinder was first shaped as carefully as possible to eliminate all original periodic errors due to the screw, the end butt, and the worm wheel. A grating of 600 lines per millimeter, ruled with the compensator in this condition, gave in the third order the spectrum of the green mercury line as shown in Figure 3 (a), a main line only

with no ghosts. When an error $a_1 \sin \theta$ was impressed on the compensator with $a_1/a_0 = 0.1274$, the result in the third order was as shown in Figure 3 (b). The main line is reduced to 0, and the first and second ghosts show on each side. When a_1/a_0 was increased to 0.203, thus making $(2\pi N a_1/a_0) = 3.832$, the result was as shown in

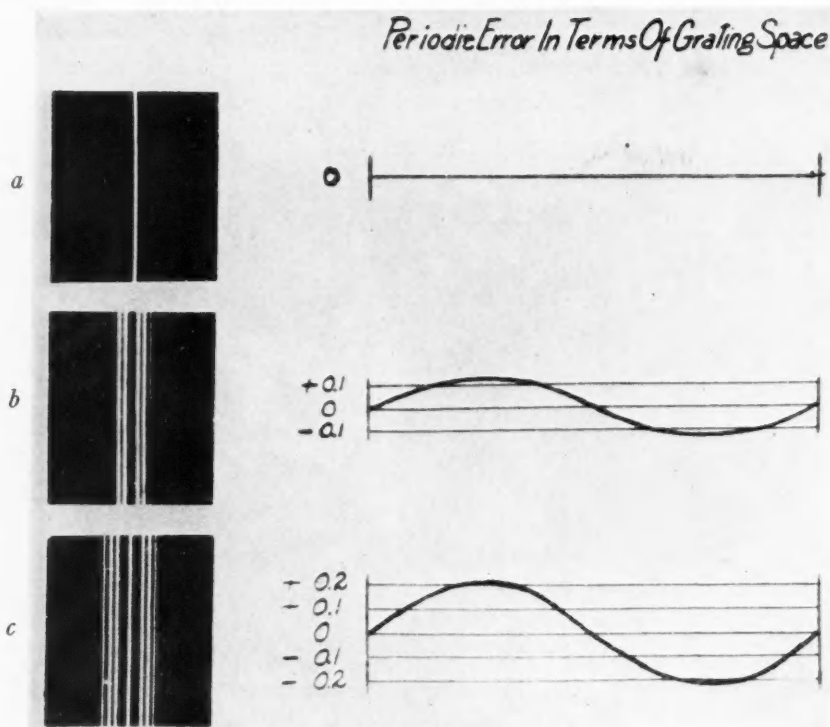


FIG. 3

Figure 3 (c). The first ghost has disappeared, and the main line and second ghost are of equal intensity, in complete agreement with theory. To secure the photographs, the gratings were placed on a spectrometer table and the eyepiece and telescope carefully focused on the lines and ghosts in question. When a small camera, focused for parallel rays, was set on the axis of the telescope, the pattern was photographed very readily.

To demonstrate the effect of the order, N , on the relative inten-

sities of the ghosts, the spectrum was photographed in the second, third, and fourth orders, with the grating which produced Figure 3 (b) above. The corresponding values of $u = 2\pi N(a_1/a_0)$ are 1.604, 2.405, and 3.208. A comparison of Figures 4 (a), (b), (c), with the table or the curves, shows how faithfully the results follow the the-

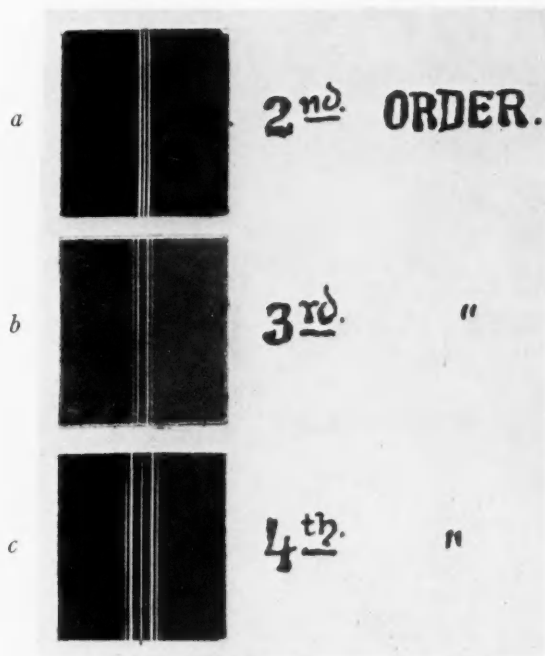


FIG. 4

ory and how badly we might be led astray in the case of strong ghosts if we followed the commonly accepted theory that the first ghost was due to an error $a_1 \sin \theta$, the second ghost to an error $a_2 \sin 2\theta$, the third ghost to an error $a_3 \sin 3\theta$, etc., since the patterns are so completely different in the different orders and only one error $a_1 \sin \theta$ is present.

Any ghost, however—for example, the third, fifth, eighth, or twentieth ghost—may be produced by impressing on the compensator an error $a \sin 3\theta$, or $a \sin 5\theta$, or $a \sin 8\theta$, etc. Errors $a \sin 8\theta$ and $a \sin 7\frac{1}{2}\theta$ impressed on the compensator gave a ghost at the

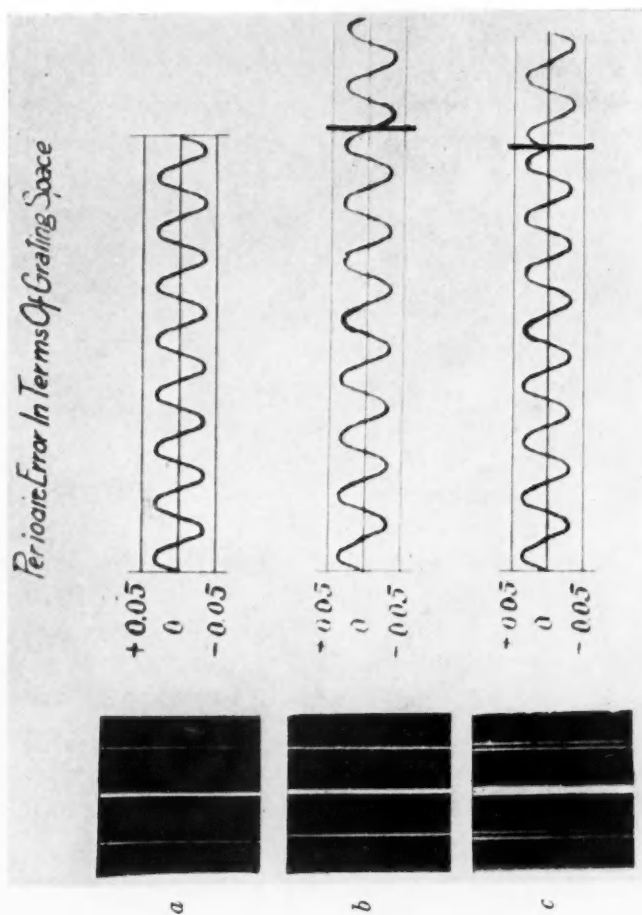


FIG. 5

position of the eighth Rowland ghosts in the first case and one at the position $7\frac{1}{2}$, midway between the seventh and eighth Rowland ghosts in the second case, as shown in Figures 5 (a) and 5 (b). However, when the error corresponding to $\sin 7\frac{1}{2}\theta$ was stopped at the end of each turn, and recommenced in the original phase, the error did not have a period corresponding to $\sin 7\frac{1}{2}\theta$ but was nearest to $\sin 7\theta +$

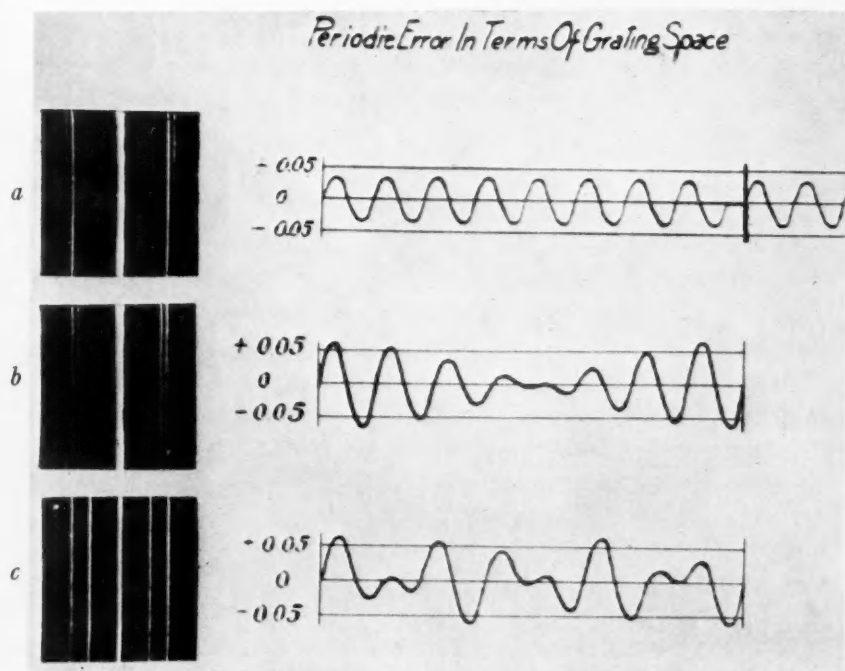


FIG. 6

$\sin 8\theta$. Ghosts of equal intensity at the positions of the seventh and eighth Rowland ghosts appeared as shown in Figure 5 (c). When an error corresponding to $a \sin 8\frac{1}{3}\theta$ was used, and started over in the original phase after each turn, ghosts appeared in the eighth and ninth positions; but the one at 8 had twice the amplitude, and therefore four times the intensity of the one at 9, as shown in Figure 6 (a). When errors corresponding to $a \sin 7\theta$ and $a \sin 8\theta$ were applied simultaneously on the compensator, equal ghosts appeared at the seventh and eighth positions, and a similar result was obtained for

errors $a \sin 5\theta$ and $a \sin 8\theta$ applied simultaneously, as shown in Figures 6 (b) and 6 (c).

As a further test, an error $a \sin 20\theta$ was used, and the twentieth Rowland ghost appeared, as shown in Figure 7 (a). When, however, the error $a \sin 20\theta$ was used on the compensator for the first half of a revolution, and no error was present for the second half, the ghosts appeared as in Figure 7 (b), a strong ghost at the position 20, with fainter ones at 19 and 21. Since the ghosts at 7 and 8 and at 5 and 8 corresponded to curves $a \sin 7\theta + a \sin 8\theta$ on the compensator in the first case, and $a \sin 5\theta + a \sin 8\theta$ in the second case, it seemed worth while to trace with the harmonic analyzer the curves $a/3 \sin 19\theta + a \sin 20\theta + a/3 \sin 21\theta$. The result is shown in Figure 8 (a), which is a fairly good first approximation to the shape of the compensator used in Figure 7 (b). Additional faint ghosts were undoubtedly present which would have been shown by longer exposure, and additional sine terms with correspondingly small amplitude would have given a closer approximation to the original curve.

Finally the error $a \sin 20\theta$ on the compensator was modified by omitting alternate loops of the curve, as in Figure 7 (c). A strong ghost appeared at position 20, with fainter ones at 10 and 30. Figure 8 (b) shows a tracing with the harmonic analyzer, using $a/2 \sin 10\theta + a \sin 20\theta + a/2 \sin 30\theta$. The reproduction of the original error curve, Figure 7 (c) is remarkably good.

The case of two periodic errors,

$$y = a_0 r + a_1 \sin e_1 r + a_2 \sin e_2 r,$$

is to be interpreted as above, a ghost appearing at the positions corresponding to e_1 and e_2 , when the errors are small. If the errors are large, the second, third, etc., ghosts due to each error will appear and will also act as principal lines for the production of ghosts by the other error, as shown in Rowland's theory. As soon as the ruling engine is available for the purpose, small gratings will be ruled with sufficiently large double periodic errors to reduce the principal line to zero and throw all the light into the ghosts. Smaller values of m will also be used to produce Lyman ghosts.

It should be borne in mind that the errors $e_1 = 2\pi/m_1$, $e_2 = 2\pi/m_2$ etc., are, in general, quite independent of the pitch of the screw. The

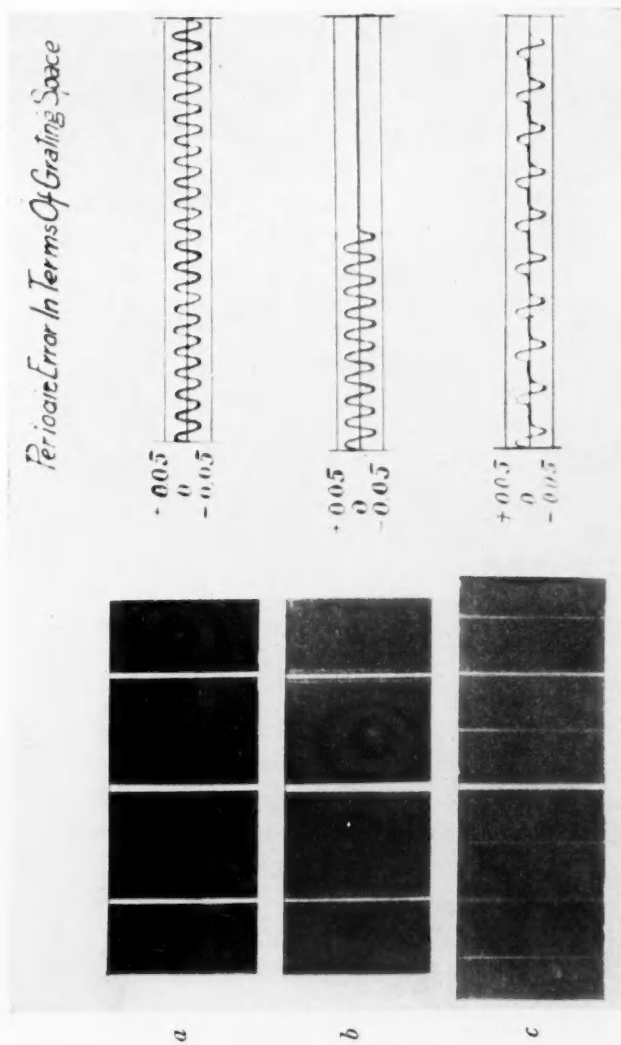


FIG. 7

number of lines, m , in a period may be fractional, and m_1 and m_2 may be incommensurable. In fact, if they are not (e.g., if $e_2 = 2e_1$), the situation becomes quite complicated, especially in the very important case of a single periodic error which is not sinusoidal. Here the natural procedure is to analyze the curve into Fourier components, and put $y = a_0r + a_1 \sin e_1r + a_2 \sin 2e_1r + a_3 \sin 3e_1r$, etc.; but even this represents the special case of a curve which is symmetrical about some point on it. The general case would demand $y = a_0r + \Sigma a_i \sin i\theta + \Sigma b_i \cos i\theta$, or its equivalent $y = a_0r + \Sigma a_i \sin (i\theta + \delta_i)$, where the δ 's are arbitrary phase constants. The case of such a periodic error is complicated, and still more so when several such errors

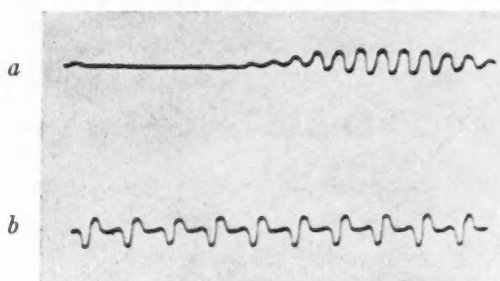


FIG. 8

are present simultaneously. Fortunately in good gratings the errors are small enough so that the first terms only in the Bessel series may be used as a sufficient approximation. Some gratings will be ruled with rather large errors of a few commensurable terms.

When numerous minor errors (probably largely typographical) are corrected, and the equations possibly extended somewhat, it is believed that Rowland's theoretical predictions will be verified.

In the Anniversary Volume dedicated to Professor K. Honda, Sendai, 1936, Siegbahn has recently published an article along lines similar to those of this article. He points out that Rowland's theory indicates that when there is an error a_i in spacing equal to one-fifth of the wave-length of sodium light in the fourth order, and there are 500 rulings per millimeter, the first ghost will be as strong as the main line. He concludes, therefore, that interferometer methods are not sufficiently accurate to correct the compensator. We have found

that we can rely on the interferometer readings to 0.1 fringe when the readings are recorded automatically and the mean is taken for several turns. With sufficient patience there is very little doubt that the errors could be determined to one-half this amount. We have used, for photographic recording of the fringes, the blue mercury line λ_{4358} . When the extreme range of the error curve is $1/10$ fringe, $a_1 = 1/20$ fringe and $a_1/a_0 = 1/(20 \times 7.6)$ since there are about 7.6 fringes to a ruling at λ_{4358} when ruling 6000 lines per centimeter. Under these conditions $2\pi N(a_1/a_0) = 0.124$.

$$J_1(0.124) = 0.0624 ,$$

$$J_1^2(0.124) = 0.0039 = 0.39 \text{ per cent} .$$

We have regularly found the ghosts less than $\frac{1}{2}$ per cent in the third order. We have ruled a number of gratings in which the first ghost in the fourth order was less than $\frac{1}{2}$ per cent of the main line.

RYERSON PHYSICAL LABORATORY
UNIVERSITY OF CHICAGO

MICROPHOTOMETRIC MEASUREMENTS IN THE SPECTRUM OF NOVA HERCULIS 1934*

PAUL W. MERRILL

ABSTRACT

The equivalent widths and residual intensities of the dark lines of component I are compared with corresponding data for α Cygni. The behavior of the D lines of sodium is exhibited by tracings in Figure 1 and the results of intensity measurements in Table 1. Data on D₃ of helium and the red Si II lines are included.

The remarkable sequence of changes in the intensity and structure of the emission lines of Fe II and [O I] is illustrated by Tables 2 and 3 and Figures 2, 3, and 4. The relationship of these changes to the magnitude of the nova and a hypothetical explanation of certain features are briefly discussed. One or two facts concerning the [N II] line λ 5755 and the unidentified line λ 6087 are given.

This investigation is supplementary to that reported in *Mt. Wilson Contr.*, No. 530. The photometric data are incomplete, being presented as samples of what can be obtained from the numerous spectrograms.

The displacements of numerous features in the green-red portion of the spectrum of Nova Herculis 1934 were discussed in *Mt. Wilson Contr.*, No. 530.¹ The photometric measurements on certain of these features, recorded in the present supplementary article, are to be regarded as sample data, a small fraction only of the material available on the numerous spectrograms having been utilized.

The fourth column of Table 1 gives the equivalent widths of several dark lines in angstrom units of total absorption; the residual intensity in the next column is the measured intensity at the bottom of the line divided by that of the adjacent continuous spectrum; while the column headed "Emission" gives the ratio of the maximum intensity of emission on the long wave-length side of the line to that of the adjacent continuous spectrum.

COMPONENT I

In the early period known as the " α Cygni" or "component I" stage, prior to the appearance of component II on December 23.5,² 1934, the sodium lines in the nova spectrum were of nearly the same

* Contributions from the Mount Wilson Observatory, Carnegie Institution of Washington, No. 563.

¹ *A. J.*, 82, 413, 1935.

² All dates are given in Greenwich Mean Time (counted from noon).

TABLE 1
MEASUREMENTS OF ABSORPTION LINES

Date	Mag.	Line	Equiv. Width	Resid. Int.	Emission
1934					
Dec. 21.56.....	1.4	D ₂ Na	0.56 A	0.75
		D ₁ Na	0.48	.79	0.08
		λ 6347 Si II	0.88	.64	0.10
		λ 6371 Si II	0.68	.72	0.07
		λ 6455 O I, Fe II	1.19	.65	0.16
		H α	2.91	.41	(1.7)
α Cygni.....	1.3	D ₂	0.58	.60
		D ₁	0.45	.68
		λ 6347	0.66	.57
		λ 6371	0.58	.63
Dec. 23.54.....	2.1	D ₂	1.20	.61
		D ₁	0.88	.68	0.15
24.09.....	2.2	D ₂	1.22	.62
		D ₁	0.87	.69	0.14
		H α	3.45	.48	0.7
25.56.....	2.9	D ₂	0.97	.72 (II) .79 (I)	0.3*
29.11.....	3.0	D ₂	(1.81)	.44	0.9*
30.10.....	2.7	D ₂	(1.13)	.59	0.8*
		λ 6347	1.21	.63	0.11
1935					
Jan. 12.09.....	2.3	D ₃ III†	0.70	.85
		D ₂ + D ₁			0.6
		λ 6347 III†	2.44	.63
		λ 6347 II	0.19	.86
		λ 6371 III†	0.80	.78
17.05.....	2.4	D ₂ + D ₁			0.8
20.03.....	2.3	D ₂ + D ₁			1.1
		λ 6347 III†	2.97	.55
		λ 6371 III†	2.01	0.67
Feb. 15.05.....	3.7	D ₂ + D ₁			(1.5)
17.98.....	3.0	D ₂ + D ₁			0.8

* Superposed emission of D₂ and D₁.

† III is used for convenience to designate any component of "large" displacement (see *Mt. W. Contr.*, No. 530, Table III).

intensity as those in α Cygni, while the two red silicon lines were considerably more intense. The residual intensities, however, were greater than those in α Cygni, showing that the nova lines were somewhat broader.

At this period the intensity ratio D_2/D_1 in the nova was 1.17. In α Cygni it is 1.29; in interstellar lines of comparable intensity, 1.2; in the sun, 1.27. For the silicon lines $\lambda\lambda$ 6347, 6371 the ratio in the nova was 1.29, while the mean value for numerous stars³ is 1.28. Since all these ratios are less than the square root of 2,⁴ it seems probable that motions of the atoms play a part in all of them.

THE SODIUM LINES D_1 AND D_2

On December 23.5, 1934, component II was visible as a very weak fringe on the violet edge of component I, and the combined intensity was considerably greater than before, while the emission was slightly more intense. Twelve hours later component II was relatively stronger, but within errors the combined intensity of components I and II was the same. On December 25.5 component II was decidedly stronger than component I (see Fig. 1), but the combined intensity was less than before. From this date on, it is difficult to obtain a significant value for the total intensity of D_1 because this line was involved in the emission of D_2 , and the true background curve upon which the absorption acts is not readily determinable. The emission maximum measured on this date, as well as on all later dates, probably included the superposed emission of D_1 and D_2 . Component I was last seen on December 26.1. The next spectrogram, on December 29.1, shows component II alone. On this date the emission was decidedly more intense than before. The apparent intensity of dark D_2 appeared to be very great, but this may possibly be a spurious result caused by drawing the background at too high a level through the influence of some emission (D_3 ?) on the violet side of the line. One day later, December 30.1, the intensity of the sodium emission was about the same, but the measured intensity of dark D_2 was considerably less. This line appeared narrower, possibly because of a change in the character of the emission

³ In α Cygni for some reason our measured value is only 1.14.

⁴ Considered the lower limit, where Doppler displacements do not enter.

on the violet side. The decrease in intensity may be intrinsic, however, at least in part, because of the related fact that lines of ionized barium, whose behavior on the whole resembled that of sodium,

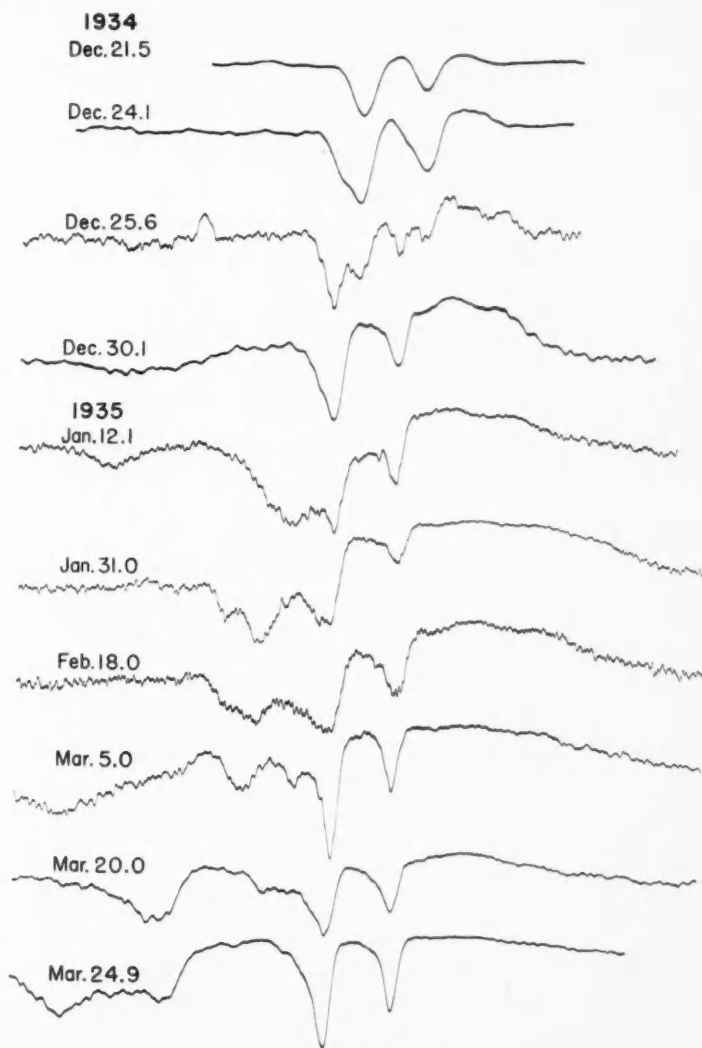


FIG. 1.—Tracings of the sodium lines D2 and D1. 1934 Dec. 21.5, component I alone; Dec. 24.1, component I with component II visible on violet side; Dec. 25.6, component II stronger than component I; Dec. 30.1, component II; the remaining tracings show component II with additional components (III) of greater displacement.

suffered a marked decline in intensity in the same twenty-four-hour interval.

On December 31.1 a new component considerably to the violet of component II was faintly present. On and after January 12.1, 1935, components with large displacements⁵ were intense, interfering so badly with component II that measurements of intensity are impracticable. Emission accompanying D₃ is an additional complicating feature.

THE HELIUM LINE D₃

On January 12.1, 1935, D₃ was a nearly symmetrical dark line 11 or 12 Å wide. Accompanying emission, if present, was of low intensity. On January 17.1 the dark line was 13 or 14 Å wide and the emission was perhaps slightly more intense. On January 20.0 both absorption and emission appeared less intense. On January 29.1 the line was broad and ill-defined. On January 31.0 and February 2.0 no absorption was present, although there was apparently a trace of emission.

EMISSION LINES

Changes in the structure and intensity of the emission lines constituted one of the most remarkable features of the spectroscopic

Date	Plate	Date	Plate
	<i>Contr. 530*</i>		<i>Contr. 530*</i>
1934 Dec. 21.6.....	Xb	1935 Jan. 17.0.....	Xh
22.6.....	XIh	20.0.....	Xi, XIc
24.1.....	Xc, XIi	21.1.....	XIm
25.1.....	Xd	31.0.....	Xj
25.6.....	XIj	Feb. 2.0.....	XId
26.1.....	Xe	18.0.....	XIe
29.1.....	Xf, XIk	Mar. 5.1.....	Xk, XI f
30.1.....	Xg, XII	17.0.....	XIn
31.1.....	XIb	25.0.....	XIg
		Apr. 2.0.....	Xl, XIo

* In *Ap. J.*, 82, 413, 1935, plate numbers corresponding to X and XI are XVIII and XIX, respectively.

history of Nova Herculis. The general character of the changes and the results of numerous position measurements were summarized in *Mt. Wilson Contr.*, No. 530.¹ More recently the intensities of three points of the wide lines have been determined from microphotom-

⁵ See *Mt. W. Contr.*, No. 530, Table III.

eter tracings of a few of the spectrograms. In Tables 2 and 3, C indicates the intensity of the continuous spectrum; M_v , M_r , and L the intensities, additional to that of the continuous spectrum, of the violet maximum, the red maximum, and the minimum near the center of the line, respectively.

For the convenience of readers who wish to refer to the illustrations in *Contr.*, No. 530 (*Ap. J.*, 82), a tabulated index is given on page 66.

LINES OF IONIZED IRON

Measurements of plates taken December 29.1 and 30.1 are shown in Table 2. Comparison of two lines, λ 5991 and λ 6516, measured on both dates, shows that the principal change was in the increased intensity of the violet maximum. The relatively high values for L and M_r of λ 6456 may be caused by the superposition of some other lines (see Fig. 2). The profiles of the iron lines resembled those of the forbidden oxygen lines on the same dates.

FORBIDDEN LINES OF NEUTRAL OXYGEN

In Table 3 the only columns needing explanation are the three headed "Mag. M_v ." The figures in these columns are the relative intensities, expressed in magnitudes, of the violet maxima, on the assumption that the intensity of the continuous spectrum near each line is represented by the stellar magnitude. While this assumption would be invalidated by changes in the general spectral energy-curve, nevertheless the three oxygen lines are probably sufficiently near the Crova wavelength for visual brightness to render the hypothesis a useful first approximation.

The auroral line was unusually faint on January 16.0 and 20.1, 1935, a fact possibly connected with the outburst of component III. Otherwise it



FIG. 2.—Tracings of emission lines of ionized iron on Dec. 30.1, 1934

seems to have remained of about the same intensity from December until the latter part of March, its variations apparently being less than those in the star's integrated light. The behavior

TABLE 2
INTENSITIES OF *Fe* II EMISSION LINES

Date	Mag.	Line	$\frac{M_V}{C}$	$\frac{L}{M_V}$	$\frac{M_R}{M_V}$	$\frac{L}{C}$	$\frac{M_R}{C}$
1934		λ					
Dec. 29.11.....	3.0	5991	0.30	0.80	0.97	0.24	0.29
		6516	.57	.67	.83	.38	.47
30.11.....	2.7	5991	.53	.46	.57	.24	.30
		6417	.30	.53	.82	.16	.25
		6433	.59	.43	.69	.25	.41
		6455	.65	(.82)	(.98)	.53	.64
		6516	0.86	0.44	0.75	0.38	0.64

TABLE 3
INTENSITIES OF [O I] EMISSION LINES

DATE	MAG.	λ 5577				λ 6300				λ 6363			
		Mag. $\frac{M_V}{C}$	$\frac{M_V}{C}$	$\frac{L}{M_V}$	$\frac{M_R}{M_V}$	Mag. $\frac{M_V}{C}$	$\frac{M_V}{C}$	$\frac{L}{M_V}$	$\frac{M_R}{M_V}$	Mag. $\frac{M_V}{C}$	$\frac{M_V}{C}$	$\frac{L}{M_V}$	$\frac{M_R}{M_V}$
1934													
Dec. 30.10.....	2.7	3.5	0.49	0.53	0.65	2.8	0.95	0.60	0.79				
1935													
Jan. 12.09.....	2.3					2.9	0.55	.77	1.09				
16.04.....	2.9	4.4	0.24	0.71	0.92								
17.05.....	2.4					2.4	0.98	.67	0.89				
20.06.....	2.3	5.0	0.08	(1.00)	(1.4)	3.1	0.46	.63	1.04				
29.05.....	2.6	3.3	0.54	0.64	0.82	2.1	1.62	.64	0.88				
31.00.....	3.4					(1.5)	(5.7)	.62	0.81	3.1	1.34	(0.78)	0.90
Feb. 11.01.....	3.0					2.3	1.88	.75	0.93	3.7	0.53		0.91
15.05.....	3.7	3.5	1.15	0.70	0.95								
17.98.....	3.0					2.6	1.52	.76	1.09	4.1	0.38	.75	1.21
19.03.....	3.4	3.8	0.68	0.65	0.85								
Mar. 5.01.....	3.7	3.8	0.90	0.40	0.84								
16.09.....	4.2					2.7	4.04	.32	0.76	4.1	1.09	(.37)	0.73
24.98.....	4.8	5.2	0.67	0.04	0.57	3.0	5.03	.17	0.58	4.7	1.11	.19	0.54
Apr. 2.01.....	5.6					(3.3)	(8.12)	.07	0.28	4.6	(2.57)	.07	0.28
1936													
Feb. 8.03.....	8.2					5.3	14.7	0.56	0.71	(6.4)	(5.1)	0.71	0.90

of the red oxygen lines also appears not to resemble that of the light-curve. These lines were relatively faint on January 20.1, when the star was rather bright, and relatively intense on January 29.0, when the star was decidedly faint. On the whole, the intensities

of these lines showed a smaller range than the light-curve. These facts suggest that the source of energy for the emission of these forbidden oxygen lines is not closely connected with the nova's visual brightness.

The ratio of intensity of the violet maximum of $\lambda 6300$ to the corresponding portion of $\lambda 6363$ was about 4 for most of the plates. On the last two plates recorded in Table 3, on which the continuous spectrum was much weaker but where the photometric data are less reliable, the value was about 3. The ratio derived by calculation is 3.⁶ The auroral line $\lambda 5577$ was less intense than $\lambda 6300$

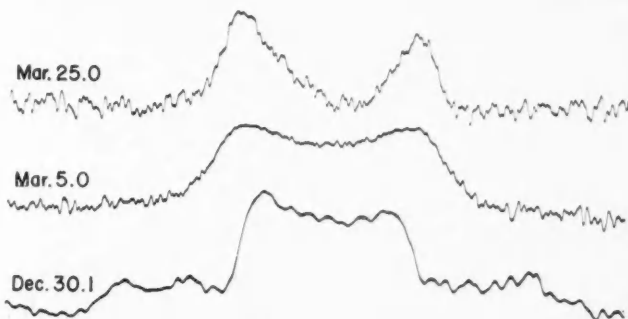


FIG. 3.—Tracings of the auroral line $\lambda 5577$, in December, 1934, and March, 1935

throughout the observed interval, beginning December 30.1, 1934. Its intensity relative to the red lines decreased markedly, with some fluctuations, from this date to March 25.0, 1935, a fact which may be interpreted as indicating a general decrease of density in the emitting gas.⁷

As might be expected, the profiles of the three forbidden oxygen lines at any given time were very much alike. Their common structure, as may be noted from Table 3, columns L/M_v and M_r/M_v , exhibited relatively little change from December, 1934, to March, 1935,⁸ when a rapid decrease began in the intensities of the center and red maxima of the lines relative to that of the violet maxima. On

⁶ E. U. Condon, *Ap. J.*, **79**, 217, 1934.

⁷ W. Grotrian, *Z. f. Phys.*, **60**, 302, 1930.

⁸ Because of the very low intensity of all portions of the line, the high values of L/M_v and M_r/M_v on January 20.1 have little significance.

April 2.0, 1935, L was only 7 per cent as intense as M_v , M_R only 28 per cent. At this time the nova had just begun an astonishing decrease in brightness. On April 10.0, magnitude 9.7, and on April 20.9, magnitude 11.3, the disparity between M_v and M_R was much greater than on April 2.0. On February 8.0, 1936, magnitude 8.2, after most of the light lost at the time of the great minimum had been regained, the structure was again more nearly symmetrical, although M_v remained more intense than M_R . A spectrogram on June 30.7, 1936, closely resembles that on February 8.0. On these dates, when

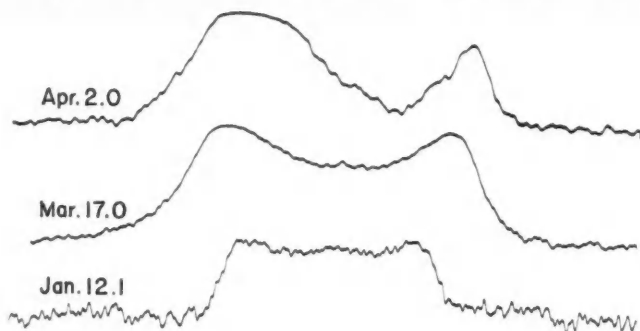


FIG. 4.—Tracings of the forbidden oxygen line λ 6300 on three dates in 1935

the magnitude was about 8, the ratios L/M_v and M_R/M_v were approximately as they had been previously when the magnitude was about 3.

A most interesting fact is that the dissymmetry of the bright lines became progressively greater as the rapid decline in brightness proceeded. The curve for M_R/M_v is approximately parallel to that for L/M_v , but displaced about 1.3 mag. toward fainter magnitudes. Since these are forbidden lines, it is not probable that the line structures were modified by atomic absorption. Either the lines were emitted as observed or some absorption not highly selective in wavelength took place. The assumption that the decreasing intensity of M_R is somehow closely connected with that of the continuous spectrum is alluring. On the hypothesis that the emitting gases moved outward from the central star either as a continuous shell or in jets, M_v would arise in front of the star, L alongside it, and M_R in the rear. Absorbing material, if placed in just the proper position,

would thus permit M_v to be less dimmed than other portions of the line. For example, under the assumption of a definitely bounded absorbing cloud advancing from one side, obscuration of jets from the star might affect the various features in the order L , M_r , C , and M_v . Hypotheses of this nature must, however, be considered in connection with numerous other facts, notably the duplicity of the star (first detected somewhat later) and the general changes in the spectrum, and preferably from a standpoint which includes oversight of the behavior of several novae.

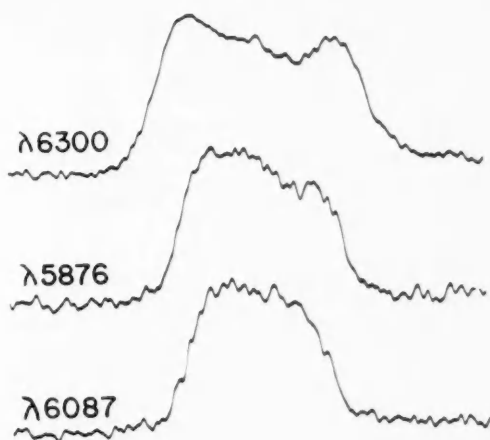


FIG. 5.—Tracings of three lines on Feb. 8.0, 1936

MISCELLANEOUS

The forbidden line of ionized nitrogen, $\lambda 5755$, was wider and more diffuse than the oxygen lines. On March 20.0, 1935, the ratios L/M_v and M_r/M_v were found to be 0.74 and 0.84, respectively, indicating that the central minimum was less pronounced than that of the oxygen lines on the same date, and that the inequality of the two maxima was less marked.

On February 8.0, 1936, the interesting line $\lambda 6087^9$ was narrower than the oxygen lines, and its structure more nearly resembled that of helium D₃ (see Fig. 5).

⁹ Adams and Joy, *Mt. W. Contr.*, No. 545; *Ap. J.*, 84, 14, 1936.

In conclusion, the incompleteness of the present measurements should be emphasized. The available spectrograms would, if desired, make possible a much more extensive investigation than the one recorded here. The data could be made more reliable by measuring unused exposures; gaps in time could be partially filled; and additional lines could be included.

CARNEGIE INSTITUTION OF WASHINGTON
MOUNT WILSON OBSERVATORY
November 1936

COMPARISON OF THE DISPLACEMENTS OF DETACHED LINES OF CALCIUM AND SODIUM IN STELLAR SPECTRA*

PAUL W. MERRILL AND ROSCOE F. SANFORD

ABSTRACT

Types B₃ and earlier.—The measured displacements of detached D₁ and D₂ agree with those of H and K in the same stars, at least to a first approximation. A slight tendency for the values from the sodium lines to be algebraically greater may be partly a regional effect.

Types later than B₃.—Comparison of sodium- and calcium-line displacements brings out the existence of blending of interstellar with stellar calcium lines in types as late as A₂.

Many years ago, several writers¹ suggested that in B-type spectra the behavior of the D lines of sodium may resemble that of the "stationary" lines H and K of ionized calcium; and in 1919 observational evidence that this is true was obtained, for a few stars, by Miss Mary L. Heger,² at the Lick Observatory. A few years later J. S. Plaskett,³ at Victoria, found that in seven O-type stars the interstellar sodium and calcium lines yield practically the same velocities.

Observations of detached lines made at Mount Wilson during the past few years now permit a comparison of the displacements of sodium and calcium lines in the spectra of numerous early-type stars. The first point to be noted is that the detached D lines are much freer from blending with stellar lines than are H and K. In O and B₀ stars the stellar calcium lines are very weak, but their intensities increase with advancing type, and interference with detached lines becomes serious at about B₃. Corresponding interfer-

* *Contributions from the Mount Wilson Observatory, Carnegie Institution of Washington*, No. 564.

¹ J. Hartmann, *Ap. J.*, **19**, 275, 1904; V. M. Slipher, *Lowell Obs. Bull.*, **2**, 1, 1909; R. H. Curtiss, *Pub. Obs. Univ. of Michigan*, **1**, 131, 1914.

² *Lick Obs. Bull.*, **10**, 59, 141, 1921.

³ *Pub. Dom. Ap. Obs.*, **2**, 338, 1923.

ence with the detached sodium lines does not begin until B8 or A0.⁴ The increased range of type includes a large number of stars and thus represents one of the principal advantages of observing the D lines.

The following computations are based on stars in whose spectra both calcium and sodium lines have been measured. We have employed, in addition to our own measurements, the interstellar velocities, mainly from the Dominion Astrophysical Observatory at Victoria, recorded in J. H. Moore's *Catalogue of Radial Velocities*.⁵

TYPES B₃ AND EARLIER

The differences between displacements yielded by calcium and sodium lines were tabulated in three groups, divided according to

TABLE 1
DISPLACEMENTS OF INTERSTELLAR LINES
(Calcium *minus* Sodium)

	WEIGHT		
	3	2	1
Number of stars.....	30	39	62
Mean arithmetical difference, km/sec..	± 2.0	± 3.2	± 4.6
Mean algebraic difference, km/sec.....	-0.7 ± 0.35	-1.3 ± 0.45	-2.4 ± 0.44

the weights of the measurements, with the results shown in Table 1. Stars in which the calcium displacement seems to be affected by a stellar component were not included. The algebraic differences, although not excessive, are several times the probable errors, and the persistence of the negative sign may be significant. The increase in the difference for observations of lower weight is a curious feature.

Figure 1 is a correlation plot of the velocities from calcium and sodium lines in types B₃ and earlier.⁶ The dotted lines on the dia-

⁴ An illustration of the greater relative intensity of the interstellar sodium lines is afforded by HD 698, classified cB8e_a (Pearce, Borsek). Pearce says (*M.N.*, 92, 884, 1932) that the interstellar K line "has an estimated intensity of 0.6 that of the stellar K line," whereas observations at Mount Wilson show that the interstellar D lines are several times as intense as the corresponding stellar lines.

⁵ *Pub. Lick Obs.*, 18, 1932.

⁶ Two later-type stars, HD 698 and U Ophiuchi, in which the interstellar lines have been observed independently of the stellar lines, are included.

gram parallel to the 45° axis are the loci of points for which calcium *minus* sodium equals ± 5 km/sec. Most of the points which lie outside the zone defined by these lines represent observations of low

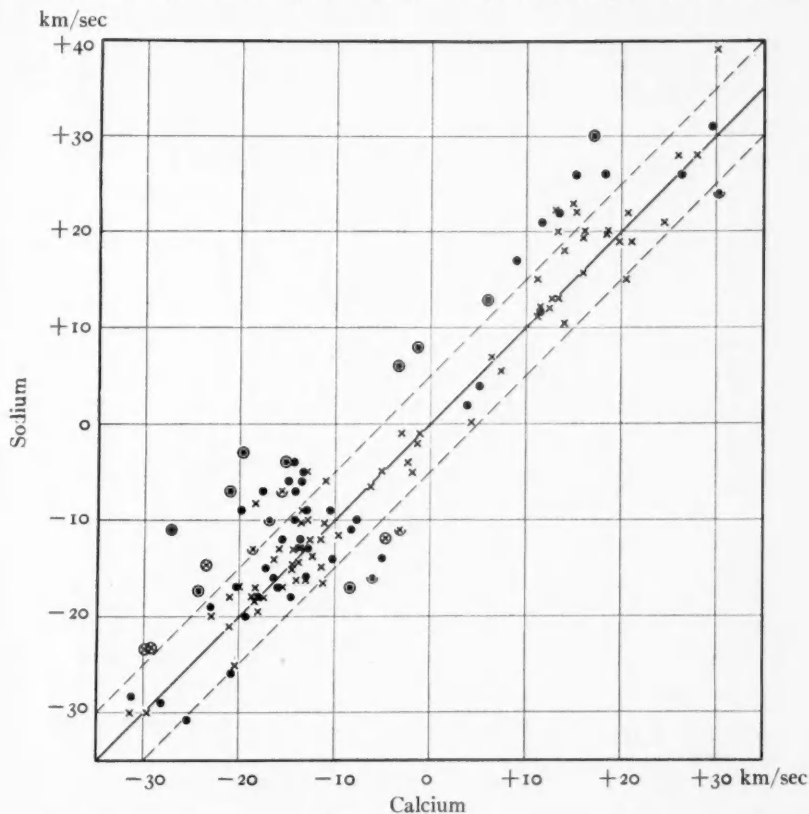


FIG. 1.—Correlation plot of radial velocities derived from calcium and from sodium lines in types B3 and earlier. Dots, observations of low weight. Dashed lines indicate differences of ± 5 km/sec relative to the 45° correlation axis. Points outside these limits for which the calcium velocity is probably affected by stellar components are marked by circles; if the effect is doubtful, a semicircle is used.

weight or stars in which the stellar calcium lines may have affected the measurements. Although the points scatter rather closely along the 45° axis, a slight preponderance occurs above and to the left.

The general conclusion is that to a first approximation the measured displacements of detached D1 and D2 agree with those of H and K in the same stars. There appears, however, a slight tendency

for the values from the sodium lines to be algebraically greater. Three possible causes of the observed differences are: (a) systematic error of measurement; (b) blending of weak stellar components with the detached calcium lines; (c) actual differences between the motions of interstellar calcium and sodium atoms.

To decide whether (b) and (c) are active, the best procedure appears to be a detailed regional study of the data—an investigation which is in progress. Preliminary results indicate that faint stars in a small area in Cygnus and a number of stars in Orion yield, for the difference calcium *minus* sodium, values of about -4 km/sec, while certain other areas give negligibly small differences.

Many of the determinations with smaller weights refer to faint stars, and the large differences might be due either to the greater distance of these stars or to some modification in the observational methods. The photographed spectra of faint stars are, in general, narrower than those of bright stars. This circumstance increases the accidental error of measurement, but we see no evidence that it introduces an appreciable systematic error. For a number of stars of weight 1 (Table 1) the sodium velocity depends on spectrograms made with the 10-inch camera instead of the 18-inch camera usually employed; but this fact appears not to be the cause of the larger algebraic difference between calcium and sodium. A tabulation of 51 stars measured with both cameras (in many instances a single plate with each) gives for the mean differences 10-inch *minus* 18-inch, arithmetic ± 3.5 , algebraic -0.5 km/sec. The algebraic difference is too small and of the wrong sign to explain the discrepancy in Table 1.

TYPES LATER THAN B₃

The failure to observe detached H and K regularly in types later than B₃ troubled investigators for many years. The explanation is now plain. In the first place stars of types later than B₃ (except the c stars) have lower absolute magnitudes than those earlier than B₃ and consequently are less distant for a given apparent magnitude. When the stars are sufficiently distant, the lines are present, although often hidden more or less completely by the stellar lines.

To exhibit the effect of blending, we have selected stars on our program of types B₅ to A₂, in which the velocity from the sodium

lines differs from the stellar velocity more than 10 km/sec. Nearly all are c stars. The relative behavior of the calcium lines is brought out by plotting the values of the differences of displacements, star

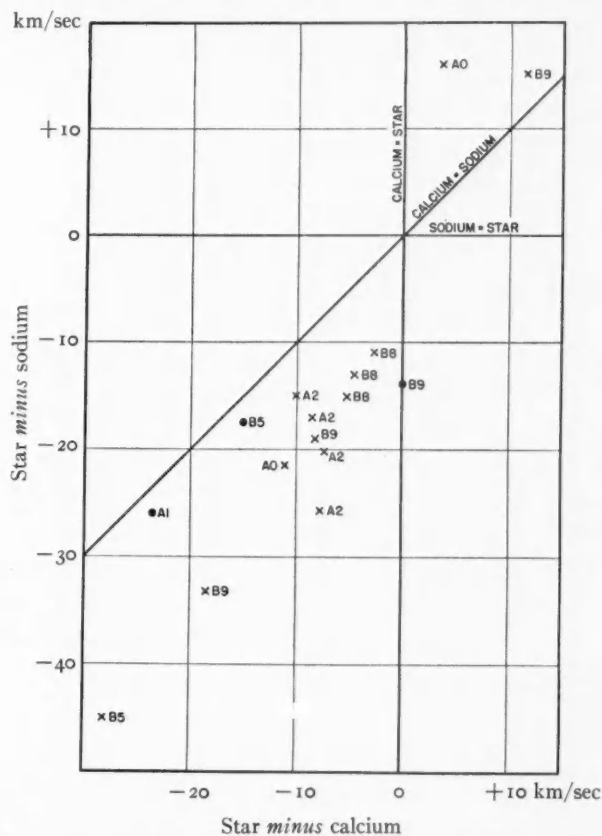


FIG. 2.—The effect of blending of stellar and interstellar components on measured displacements of the H and K lines in types later than B3. Dots, observations of low weight.

minus calcium, as abscissae against star *minus* sodium as ordinates (see Fig. 2). It is obvious that stars whose calcium velocities are equal to the stellar velocities will be represented by points on the y-axis; if the calcium velocities are equal to the sodium velocities, the points will lie on a 45° line through the first and third quadrants. Intermediate calcium velocities will correspond to points in the

second halves of the first and third quadrants. Inspection of the diagram shows that the plotted points do actually lie in these sectors. This exhibits the influence of blending in types as late as A2.

Since the velocity of interstellar matter is, to a certain extent, a function of distance, the data on displacements of interstellar lines make it highly probable that throughout the galactic regions under observation the motions of sodium and calcium atoms are, with possible minor exceptions, similar, and that the densities are nearly proportional.

CARNEGIE INSTITUTION OF WASHINGTON
MOUNT WILSON OBSERVATORY
December 1936

NEW IDENTIFICATIONS OF SOLAR LINES*

CHARLOTTE E. MOORE

ABSTRACT

A summary of elements present in the solar spectrum is discussed. The 92 chemical elements are divided into five groups as follows: 61 present; 3 possibly present (*Sn*, *Ta*, *Tb*); 2 having insufficient solar data (*Ne*, *Cs*); 7 having insufficient laboratory data; 19 absent.

Over 400 faint new lines have been measured between λ 6600 and λ 7330 as part of Mr. Babcock's work on the infrared solar spectrum. Among these, the two *Li* lines at λ 6707, previously found only in the spot spectrum, have been measured in the spectrum of the disk (intensity -3). Similarly, the stronger *Rb* line λ 7800 is also present in the disk spectrum.

Os and *Ir* may now be classified as present without question. Their presence has previously been suspected but not confirmed. *Tu* has been detected for the first time. It occurs only in the ionized state, like most of the rare earths. Laboratory material has been lacking for this element until recently.

Three elements, *Sn*, *Ta*, and *Tb*, must remain as doubtfully present. Laboratory measures are needed for *Sn* and *Tb*. The three strongest *Ta* lines agree with faint solar lines recorded by Rowland, but the reality of two of the solar lines is somewhat questionable.

The strongest accessible line of *Ne* is suspected to be present in the chromosphere, but further measures are needed for confirmation of its presence. For *Cs*, the infrared sun-spot spectrum must be adequately photographed before any statement can be made as to its presence or absence.

Of the 7 elements with insufficient laboratory data, the spectra of *Th*, *U*, and *Ho* may be observed in the near future. The remaining 4 elements *Ma*, 85, 87, and *Il*, have not been isolated in sufficient quantity, if at all, to make this possible.

The 19 absent elements are listed in order of excitation potential of the accessible lines, except for the radioactive elements, which are not to be expected.

The photography of the solar spectrum in the infrared, by Mr. Babcock at Mount Wilson, has had an interesting bearing on our knowledge of the elements present in the sun. Although the work in the region $\lambda\lambda$ 6600-13,500 (the present limit) is not completed yet, a summary of the identifications to date may not be amiss.

From spectroscopic evidence the 92 chemical elements may be divided into five classes for the purpose: (1) present; (2) doubtfully present; (3) insufficient solar data; (4) insufficient laboratory data; (5) absent. The results to date are as follows:

Present.....61	Present?.....3	Insufficient solar data.....2
Insufficient laboratory data.....7	Absent.....19	

* Contributions from the Mount Wilson Observatory, Carnegie Institution of Washington, No. 565.

The elements arranged according to these groups are given in Table 1. Those listed as absent are subdivided into three classes, namely, those with accessible ultimate lines, those with inaccessible ultimate lines, and those which are radioactive and therefore not to be expected. The excitation potentials of the strongest available lines are entered above the element for this group.

TABLE 1
ELEMENTS IN THE SUN

		$\left\{ \begin{array}{l} H\ He\ \underline{Li}\ Be\ B\ C\ N\ O\ F\ Na\ Mg\ Al \\ Si\ P\ S\ K\ Ca\ Sc\ Ti\ V\ Cr\ Mn\ Fe\ Co \\ Ni\ Cu\ Zn\ Ga\ Ge\ \underline{Rb}\ Sr\ Y\ Zr\ Cb\ Mo \\ Ru\ Rh\ Pd\ Ag\ Cd\ In\ Sb\ Ba\ La\ Ce \\ Pr\ Nd\ Sa\ Eu\ Gd\ Dy\ Er\ \underline{Tu}\ Yb\ Lu \\ Hf\ W\ \underline{Os}\ \underline{Ir}\ Pt\ Pb \end{array} \right.$
Present	61	
Present?	3	$\underline{Sn}\ \underline{Ta}\ \underline{Tb}$
Insufficient solar data	2	$\underline{Ne}\ \underline{Cs}$
Insufficient laboratory data	7	$Ma\ (Sn)^* 85\ 87\ \underline{Th}\ \underline{U}\ \underline{Il}\ (\underline{Tb})\ \underline{Ho}$
Absent	19:	
Ultimate lines accessible	3	$\left\{ \begin{array}{l} 0.0\ 0.0\ 0.0\ 0.0\ 0.0 \\ (Cs)\ Re\ Tl\ Bi\ (Ra) \end{array} \right.$
Ultimate lines inaccessible	11	$\left\{ \begin{array}{l} 2.3\ 4.6\ 4.9\ 5.5\ 6.0\ 6.9 \\ As\ Au\ Hg\ Te\ Se\ I \\ 7.8\ 8.3\ 8.9\ 9.9\ 11.5\ 16.6 \\ Br\ Xe\ Cl\ Kr\ A\ (Ne) \end{array} \right.$
Not to be expected	5	$Po\ Rn\ Ra\ Ac\ Pa$

* Parentheses denote that element is entered twice.

The present paper deals chiefly with the elements which are underlined in Table 1: *Li, Rb, Tu, Os, Ir; Sn, Ta, Tb; Ne, Cs; Th, U, Ho.*

ELEMENTS PRESENT

It has been previously supposed that lines of *Li* and *Rb* were present only in the sun-spot spectrum. New red-sensitive plates taken with the tower telescope at Mount Wilson indicate that many faint lines are present from $\lambda\ 6600$ to $\lambda\ 7330$ (the limit of Rowland's plates) which were not recorded by Rowland. Over four hundred

additional lines have recently been measured. They are extremely faint and difficult to see, and most of them have been measured on only one plate. In order to check their reality, measures should be made on two plates taken with different gratings. It is not certain that this can be done in time for the publication of the *Infrared Solar Spectrum*, but there is apparently a wealth of new material available. Among these lines Babcock has measured two at λ 6707.76 and λ 6707.98. The *Li* spot lines are at λ 6707.77 and λ 6707.94.

Similarly, the leading line of the *Rb* pair at λ 7800.29 agrees with a line of intensity -3 measured in the disk spectrum at λ 7800.32. Both *Li* and *Rb* may therefore possibly be present very faintly in the solar spectrum.

The three elements *Os*, *Ir*, and *Tu* are, for the first time, here classified as present. Recent accurate measures of the ultimate lines of *Os* and *Ir*, made by W. S. Albertson, of the Massachusetts Institute of Technology, have made it possible to determine the presence of *Os* and *Ir*, which have previously been in the questionable list.

The evidence for *Os* is given in Table 2. The first five columns contain the laboratory data: wave-length, intensity, lower excitation potential, inner quantum numbers, and multiplet designations, respectively. The last four columns give the solar data: wave-length, intensity, $\Delta\lambda$ (Sun-Laboratory), and suggested identification of the solar line. An accurate measure of the strongest available ultimate line, λ 4135, is 0.019 Å to the red of a solar line of intensity 0. All other leading lines are blended, masked, or doubtfully present; but on the evidence afforded by this line it may reasonably be assumed that *Os* is present.

During the preparation of the *Revised Rowland Table*¹ a search for *Ir* was made in the solar spectrum; but, owing to insufficient data, no lines were attributed to this element. In the *Multiplet Table*² two faint solar lines were identified with question as *Ir*, but the apparent absence of a *raie ultime* at λ 3513.67 cast grave doubt upon the correctness of the identifications. Recent work on the analysis of *Ir*,³ based on revised accurate laboratory wave-lengths,

¹ Carnegie Inst. of Wash. Pub., No. 396; *Papers of the Mt. W. Obs.*, 3, 1928.

² Princeton, 1933.

³ Albertson, unpublished material.

now indicates that the strongest available ultimate line is present in the solar spectrum, giving a line of intensity -2. Of the next strongest ultimate lines to the red of λ 2975 (the violet limit of the solar spectrum), one is masked in the sun; one is blended with *Cr*; and the third has been remeasured at λ 3513.638, which is 0.033 Å to

TABLE 2
OSMIUM IN THE SOLAR SPECTRUM

LABORATORY*					SUN				
I.A.	Int.	Lower E.P.	I.Q. Nos.	Desig.	I.A.	Intensity		$\Delta\lambda$ (☉-Lab.)	Solar Ident.
						Disk	Spot		
4135.784†	30	{ 0.513 1.740	3-4 3-3	3 - 32° 13 - 60°	.765	0	2§	-019	-Os
4211.90	30	2.897	5-5	27°-103	.891	2	2	-01	Zr ⁺ -Os
3752.54	20R	0.338	2-3	2 - 35°	.508	-2	-03	Nd ⁺ -Os
3782.19	20R	0.513	3-4	3 - 39°	.220	0	+03	CN Os?
4112.04	20	0.712	1-2	5 - 36°	1.988	-2	-1N	-05	-Os??
4260.85	20	0.000	4-5	1 - 27°	.840	0	-2?	-01
4420.47	20	0.000	4-4	1 - 26°	.46	-1	-01	Zr?-Os?
3793.93	15	2.333	3-2	20 - 94°	.972	-2	+04	Sa ⁺
3903.65	15	0.513	3-3	3 - 35°	.695	3	4	+04	Cr
3977.24	15	0.635	5-5	4 - 37°	.198	0	0	-04	Co
4173.24	15	0.635	5-6	4 - 34°	Absent
3267.96	10R	0.000	4-4	1 - 39°	Absent
3301.56	10R	0.000	4-5	1 - 37°	.580	-3	+02	Os??
3058.68	8R	{ 0.000 1.740	4-4 3-3	1 - 41° 13 - 101°	.707	0	+03	Os??

* Albertson, *Phys. Rev.*, **45**, 304, 1934.

† Albertson, communicated by letter, December, 1936.

§ Blend.

the red of a faint solar line which may be due partly to a predicted line of *Fe*. The error in the older measures of this line led to the conclusion that it was absent from the solar spectrum. Of the eleven remaining strong low-level lines of *Ir*, four are possibly present, five are masked or otherwise identified in the sun, and two are absent.

The results are summarized in Table 3, which is arranged similarly to Table 2. From the data contained in Table 3 it may reasonably be

concluded that *Ir* is present, although faint in the sun. Probably no lines of laboratory intensity less than 60 are present.

TABLE 3
IRIDIUM IN THE SOLAR SPECTRUM

LABORATORY					SUN			
I.A.	Int.	Lower E.P.	I.Q. Nos.	Multiplet Desig.	I.A.	Int.	$\Delta\lambda$ (\odot -Lab.)	Solar Ident.
2882.624	60	0.350	41-31	b ⁴ F-z ⁴ D ⁰ †
3198.917	60	0.877	31-21903	-2N	-0.014	Fe?
3287.584	50	0.877	31-31584	-3	.000	Co?
2849.724	80	0.000	41-41	a ⁴ F-z ⁶ G ⁰ †
2924.783	100	0.000	41-51
3437.006†	60	0.781	31-31055	3	+ .049	Fe
2936.678	50	0.504	11-11	a ⁴ F-z ⁶ F ⁰ †
2951.222	50†	0.000	41-31
3241.510	50	0.504	11-21490	0	- .020	Fe
3266.446	60	0.714	21-11440	-1d?	- .006	Ti ⁺ -Ir?
3513.638†	80	0.000	41-51605	-2	- .033	Fe-Ir?
2824.444	60	0.350	41-41	b ⁴ F-z ⁴ G ⁰ †
3177.570	50	0.877	31-31543	2	- .027	Fe ⁺
3212.121	60	0.877	31-41166	1	+ .045	Fe
3068.807	60	0.350	41-31	b ⁴ F-z ⁶ G ⁰ †	Absent
*3915.384	60	1.219	21-31	Absent
3220.772†	100	0.350	41-31	b ⁴ F-z ⁶ F ⁰ †	.776	-2	+ .004	Ir
3368.472	60	0.350	41-41446	-3	- .026	Fe ⁺ ?
3902.503	50	0.350	41-51	Absent
*3934.833	50	0.877	31-41	Absent
3992.114	80	0.877	21-21118	-1	+ .004	Ir?-Cr
3448.967	60	0.504	11-21	a ⁴ F-z ⁶ D ⁰ †	.965	-3	- .002	Ir?
3522.020	50	0.504	11-11045	-3	+ .025	Nd ⁺
3800.122	60	0.000	41-41115	0	- .007	CN
4268.096	80	0.877	31-31	b ⁴ F-z ⁶ D ⁰ †	.114	1N	+ .018	§
4311.500	50	1.219	21-21515	2*	+ .015	CH
*3915.384	60	1.599	21-11	D-z ⁴ D ⁰	Absent
*3934.833	50	1.599	21-21	Absent
4069.912	60	1.599	21-31906	-2	- .006	Ir?
3976.306	60	1.616	31-41	E-z ⁴ G ⁰	.278	-1	-0.028	Sa ⁺ ?-Ir?

* Blend.

† Raie ultime?

‡ Multiplet incomplete; remaining lines too faint to be considered here.

§ Masked.

Tu can now be listed as present in the ionized state in the solar spectrum. Previously the data have been insufficient to determine either its presence or its absence. From recent unpublished laboratory material by W. F. Meggers and A. S. King, the 11 strongest *Tu*⁺ lines (intensity 150 and greater) are well measured and can be accounted for in the solar spectrum as follows: 3 unblended; 1 unblended(?); 3 blended; 4 masked. A fainter line at λ 3701 may also

TABLE 4
THULIUM IN THE SOLAR SPECTRUM

LABORATORY*				SUN				
I.A.	Intensity		Temp. Class.†	I.A.	Intensity		$\Delta\lambda$ (\odot -Lab.)	Solar Ident.
	Arc	Spark			Disk	Spot		
3131.26	300	300237	0	-0.02	<i>Cr-Tu</i> ⁺
3151.03	150	150006	1	-.02	<i>OH</i>
3172.81	150	150	III E	.853	-2	+.04	<i>Tu</i> ⁺ ?
3362.61	200	200594	-3	-.02	<i>Tu</i> ⁺
3425.08	150	200064	-2	-.02	<i>V Tu</i> ⁺
3462.20	200	200	III E	.214	-2	+.01	<i>Tu</i> ⁺
3701.34	100	60	III E	.376	-2	+.04	<i>Tu</i> ⁺ ? <i>Mn</i> ⁺ ?
3761.33	200	150322	7	-.01	<i>Ti</i> ⁺
3795.76	250	200745	-1	-.02	<i>CN</i>
3848.03	350	300	III E	.053	-1	+.02	<i>CN Tu</i> ⁺
4522.57	250	300527	0	0	-.04	<i>Fe</i>
4615.95	200	200940	-1	-0.01	<i>Tu</i> ⁺

* Meggers, unpublished material, December, 1936.

† King, unpublished material, December, 1936.

be present. The ionization potential is probably low, and consequently *Tu* is probably present only in the ionized state, as are most of the rare earths. The data are given in Table 4.

ELEMENTS DOUBTFULLY PRESENT

The identification of *Sn* in the solar spectrum is unusually difficult and interesting. Six low-level lines are in the accessible region. Of these, two are masked by strong lines of *Fe*; one has been identified in the solar spectrum as *Fe-Fe*⁺, but Burns suspects that the *Fe* line may be a *Sn* impurity in the *Fe* spectrum; one may be masked by *Cr*, but the laboratory wave-length of *Sn* is inaccurate and no

calculated wave-length can be obtained from multiplet data. The remaining two lines are weaker and have higher excitation potentials, but they coincide with solar lines of intensity -2 , one of which may be due to *NH*. Accurate laboratory measures of a pure *Sn* spectrum are needed before any decision as to the presence or absence of the element can be made. The best available measures were made in 1914. Therefore, this element must still remain in the class of those whose presence is questionable. The data are given in Table 5.

TABLE 5
TIN IN THE SOLAR SPECTRUM

LABORATORY					SUN			
I.A.	Int.	Lower E.P.	I.Q. Nos.	Multiplet Desig.	I.A.	Int.	$\Delta\lambda$ (\odot -Lab.)	Solar Ident.
3009.138	50R	0.209	1-1	$a^3P-z^3P^{*}$.090	1	-0.048	<i>Fe</i>
3034.16	50R	0.209	1-0		.201	2	+ .04	<i>Cr</i>
3034.116					.063	-1	- .053	
3175.039	100R	0.423	2-1		.046	0	+ .007	<i>Fe†-Fe+</i>
3262.338	100R	1.063	2-1	$a^1D-z^1P^0$.289	3	- .049	<i>Fe</i>
3330.596	20	1.063	2-2	$a^1D-z^3P^0$.616	-2	+ .020	<i>Sn? NH</i>
3801.031	30R	1.063	2-1		.027	-2	-0.004	<i>Sn?</i>

* Rest of multiplet to violet of λ 2975.

† Line attributed to *Fe* may be a *Sn* impurity in *Fe* spectrum (Burns).

The three strongest low-level lines of *Ta* coincide with solar lines of intensity -3 measured by Rowland and entered in the *Revised Rowland Table*. Upon this evidence *Ta* was listed by Kiess⁴ as present in the sun. Later Babcock discovered that the two of longer wave-length might possibly be ghosts, and this leaves the presence of *Ta* open to some question. Other coincidences of fainter laboratory lines with solar lines may or may not be accidental. The three *Ta* lines in question are absent from the spot spectrum. The data are given in Table 6.

The presence of *Tb* must remain questionable until better laboratory material is available. Many of the strongest lines of *Tb*⁺ are masked in the solar spectrum, but some are absent. Some of the

⁴ *Bur. of Standards J. of Res.*, **12**, 459 (RP 671), 1934.

strongest lines may be present in the flash spectrum, but some are absent, and for others the discordance in wave-length is considerable. If present, *Tb* must exist only in the ionized state.

ELEMENTS WITH INSUFFICIENT SOLAR DATA

The presence of the strongest available line of *Ne*, λ 6402.2455 (E.P. 16.6) is suspected in the chromosphere, according to Menzel.⁵ An extremely faint trace is visible near λ 6402, but its wave-length is not accurately known. Further measures are necessary before its presence can be determined.

TABLE 6

LABORATORY					SUN			
I.A.	Int.	Lower E.P.	I.Q. Nos.	Desig.	I.A.	Int.	$\Delta\lambda$ (\odot -Lab.)	Solar Ident.
5939.75	20b	I. 205	$\frac{1}{2}$ -1 $\frac{1}{2}$	⁶ D-W ^o	.754	-3	0.00	<i>Ta?</i>
5944.01	30d?	I. 232	1 $\frac{1}{2}$ -2 $\frac{1}{2}$	⁴ D-W ^o	.017	-3	+ .01	<i>Ta?</i>
5997.24	35c	I. 648	4 $\frac{1}{2}$ -4 $\frac{1}{2}$	⁶ D-V ^o	.223	-3	-0.02	<i>Ta?</i>

It is possible that *Cs* may be present, but the ultimate lines lie at λ 8521 and λ 8943. If present, lines of this element will appear only in the sun-spot spectrum, on account of its low ionization potential (3.88). No adequate spot spectrum exists in this region, but it is hoped that plates will be taken during the coming sun-spot maximum. The lines are absent from the existing plates.

ELEMENTS WITH INSUFFICIENT LABORATORY DATA

It should be possible to secure good laboratory data for *Th*, *U*, *Tb* and *Ho* within a reasonable length of time. The presence of these elements can then be discussed. Nothing is known at present about the spectra of *Ma*, 85, 87, and *Il*.

ABSENT ELEMENTS

In a discussion of the composition of the sun's atmosphere, Russell⁶ states that "it appears that the principal factor which is un-

⁵ Communicated by letter, December, 1936.

⁶ *Mt. W. Contr.*, No. 383, 25; *A p. J.*, 70, 35, 1929.

favorable to the appearance of a spectral line in the sun is a high excitation potential." The elements which are absent are arranged in Table 1 in order of the excitation potential of accessible lines. Those with low excitation potential must be entirely too rare to be detected spectroscopically (*Re, Tl, Bi*). For *As* the test is much less delicate, since intersystem combinations are involved. The excitation potentials are unfavorable for the detection of the others.

The present report has been made possible only through the generous co-operation of several institutions. The writer is extremely indebted to Messrs. Walter Albertson of the Massachusetts Institute of Technology, W. F. Meggers and C. C. Kiess of the Bureau of Standards, D. H. Menzel of Harvard, and A. S. King of Mount Wilson for valuable unpublished material. She is also very grateful to Mr. Russell for his keen interest and many helpful suggestions.

PRINCETON UNIVERSITY OBSERVATORY,
CARNEGIE INSTITUTION OF WASHINGTON
MOUNT WILSON OBSERVATORY

December 24, 1936

HYDROGEN EMISSION IN THE CHROMOSPHERE

D. H. MENZEL AND G. G. CILLIÉ

ABSTRACT

Intensities of the Balmer series are given up to H_{31} and of the continuous spectrum beyond, as observed for the 1932 chromosphere. The relative intensities of lines lying near together in the spectrum, like the upper members of the Balmer series, are probably close to the truth. For lines lying far apart, like $H\alpha$ and H_{31} , the relative intensities are subject to greater uncertainty.

From the intensities in the Balmer continuum at λ 3640 and λ 3500 a temperature of about 10,000° for the free electrons in the chromosphere is deduced.

From the intensities of $H\alpha$ – H_{31} the relative numbers of hydrogen atoms in the various excited states can be derived. Beyond H_{31} the series members merge to form a continuum that grades without discontinuity into the true Balmer continuum at λ 3647.4. From the intensity of this spectrum the population of states above the thirty-first can be derived. These numbers are compared with those in an inclosure in thermodynamic equilibrium, containing the same numbers of electrons and protons and at the temperature of the free electrons in the chromosphere. It is found that for states above the twentieth the populations in the chromosphere and in the thermodynamic inclosure are indistinguishable. For lower states the chromosphere seems to show a relative deficiency of population.

The populations of states of large-quantum number in a purely capture spectrum are computed, from which figures the theoretical Balmer decrement may be calculated. It is found that the populations are of the order of one-half of the observed populations for the chromosphere. It appears probable that the chromospheric hydrogen spectrum arises from line excitation as well as from electron capture. Hydrogen emission in the chromosphere apparently cannot be explained by the action of excess radiation in the extreme ultraviolet, far beyond the Lyman limit.

I. INTRODUCTION

On the objective-prism spectrograms obtained by the Crocker Expedition of the Lick Observatory at the August, 1932, eclipse¹ the Balmer lines as far as H_{31} are resolved. From the relative intensities of these lines, E_n , and the theoretical Einstein transition probabilities, A_{n2} , the relative numbers of hydrogen atoms in the various excited states, N_n , in the chromosphere can be derived. The members beyond H_{31} merge into a continuous spectrum, partly because of the lack of instrumental resolving power and partly because, beginning at a certain point near the ionization limit, the hydrogen states broaden and overlap. From the intensity distribution in this spectrum it is possible to determine the populations of the states above the thirty-first.

¹ *Pub. A.S.P.*, **44**, 341, 1932.

On some of the spectrograms the continuous emission at the head of the Balmer series—which grades without a noticeable discontinuity into the above-mentioned continuous spectrum—is very prominent. This emission arises from the capture of free electrons in the second-quantum state of hydrogen, and its intensity distribution depends upon the velocity distribution of the free electrons. This fact is used to determine the electron temperature in the chromosphere.

The populations of the higher states of hydrogen in a purely capture spectrum—i.e., one in which the emission arises from electron capture only and where line excitation plays no part—are computed. These populations are compared with the observed ones for the chromosphere, and it is then possible to decide to what extent line excitation is responsible for the chromospheric hydrogen emission.

2. INTENSITIES OF THE BALMER LINES

Table 1 gives the intensities determined from chromospheric spectra made with the ultraviolet spectrograph (*UV*); Table 2 gives those determined from spectra made with the grating spectrograph (red). The former covered the range $\lambda\lambda$ 3300–5300, and the latter the range $\lambda\lambda$ 3750–6600.

Intensities were determined by measuring areas under line profiles derived in the usual manner from microphotometer tracings and characteristic curves. For each set of films one characteristic curve was used throughout the wave-length range. In the case of the *UV* films a single standardization, obtained with a step wedge and a violet light-source, was available. Evidence against a change of characteristic curve with wave-length in the region under consideration is the absence of any systematic effect in the emission gradients of the metallic lines, as determined from successive members of the film series. For the red films three characteristic curves obtained with red, orange, and yellow light-sources were found to be indistinguishable and were combined into a single curve, which was also used in the violet region.

We have attempted to correct the intensities for the differential effects of the atmosphere, the instrument, and the photographic plate, and to reduce them to absolute units. The continuous spectra

TABLE 1
THE BALMER DECREMENT (UV SPECTROGRAPH)

λ (Int.)	El.	$\log E_{49a}$ (670 km)	$\log E_{48a}$ (1500 km)	$\log E_{49b}$ (900 km)
4861.3 (100).....	$H\beta$	15.76*	15.34*	15.90*
4340.5 (85).....	$H\gamma$	15.17*	14.74*	15.31*
4101.8 (75).....	$H\delta$	14.83*	14.41*	14.97*
3835.4 (55).....	H_9	14.35*	13.91	14.49*
3834.3 (7).....	Fe			
3797.9 (50).....	H_{10}	14.11*	13.67	14.25*
3797.8.....	CN			
3770.6 (50).....	H_{11}	14.05*	13.61	14.19*
3750.2 (45).....	H_{12}	14.02*	13.58	14.16*
3749.5 (6).....	Fe			
3734.9 (3).....	Fe	13.98*	13.53	14.12*
3734.4 (40).....	H_{13}			
3721.9.....	H_{14}	13.88*	13.43	14.02*
3721.6 (35).....	Ti^+			
3712.0 (30).....	H_{15}	13.80	13.33	13.94*
3711.9.....	$FeZr^+$			
3703.9 (25).....	H_{16}	13.74	13.25	13.88*
3697.2 (20).....	H_{17}	13.69	13.23	13.83*
3696.7 (2).....	Ni			
3691.6 (15).....	H_{18}	13.60	13.17	13.74*
3686.8 (10).....	H_{19}	13.58	13.11	13.72*
3682.8 (8).....	H_{20}	13.51	13.01	13.65*
3682.7 (2).....	Zr^+			
3679.9 (3).....	Fe	13.50	12.99	13.67
3679.4 (8).....	H_{21}			
3676.4 (6).....	H_{22}	13.40	12.92	13.57
3674.1 (3).....	$NiFe$	13.40	12.87	13.52
3673.8 (5).....	H_{23}			
3671.4 (5).....	H_{24}	13.31	12.78	13.49

* These values in Tables 1 and 2 do not represent direct measurements, the lines being overexposed on the films in question. They are obtained from measurements on earlier members of the film series and from the measured emission gradients in the chromosphere.

TABLE 1—Continued

λ (Int.)	El.	$\log E_{49a}$ (670 km)	$\log E_{48a}$ (1500 km)	$\log E_{49b}$ (900 km)
3669.5 (5).....	H_{25}	13.28	12.71	13.44
3669.4.....	V^+			
3668.0 (2).....	Ce^+	13.26	12.67	13.40
3667.7 (4).....	H_{26}			
3666.5 (2).....	Sc^+	13.20	12.62	13.30
3666.1 (4).....	H_{27}			
3664.7 (4).....	H_{28}	13.17	12.63	13.32
3664.6.....	V^+			
3663.5 (2).....	Fe	13.10	12.55	13.25
3663.4 (1).....	H_{29}			
3662.3 (7).....	H_{30}	13.23	12.57	13.35
3662.2.....	Ti^+			
3661.4 (1).....	$FeSa^+$	13.05	13.09
3661.2(-1).....	H_{31}			

from the chromosphere itself and from the extreme limb of the sun—up to one-thousandth of the radius from the edge—are recorded and are measurable on different members of the film series.

TABLE 2

THE BALMER DECREMENT (GRATING SPECTROGRAPH)

λ (Int.)	El.	$\log E_{49a}$ (670 km)	λ (Int.)	El.	$\log E_{49a}$ (670 km)
6562.8.....	$H\alpha$	16.46*	3835.4 (55)....	H_9	14.31
4861.3(100).....	$H\beta$	15.54*	3834.3 (7)....	Fe	
4340.5 (85).....	$H\gamma$	14.97*	3797.9 (50)....	H_{10}	14.09
4101.8 (75).....	$H\delta$	14.72	3797.8.....	CN	
3970.1.....	$H\epsilon$	14.57	3770.6 (50)....	H_{11}	13.97

* See note to Table 1.

All films were exposed for the same length of time at regular intervals during the progress of the eclipse. In view of the uncertainty with regard to the intensity distribution in these spectra, especially

in the ultraviolet region, we assumed that the distribution in the continuous chromospheric spectrum is the same as that of a black body at 5700° , and that the continuous spectrum from the extreme edge is that of a black body at 4700° . There is evidence in favor of a lower temperature at the extreme limb in the observations by Abbot, Fowle, and Aldrich² of the darkening toward the limb of the sun.

Our resultant absolute intensities are in satisfactory agreement with those of Pannekoek and Minnaert, as far as they can be compared.³ Full details of this comparison, as well as of the standardization, have been published elsewhere.⁴

It is sufficient to point out here that the relative intensities of lines spread over a small region of the spectrum, as for instance those of the lines H_9 - H_{31} , are probably close to the truth. For lines as widely separated as $H\alpha$ and H_{31} the relative intensities are subject to much greater uncertainty.

In column 1 of Tables 1 and 2 are given the wave-lengths and intensities of the lines of the Balmer series, as well as those of lines blended with them which may contribute to the intensity. These identifications are quoted from results obtained at the 1905 eclipse.⁵ Evidently the metallic lines were not so strong for the observations of 1932 as for those of 1905. No corrections for blending were applied to the 1932 measurements, and only in the case of H_{30} is blending of sufficient importance to warrant the exclusion of the line from further discussion.

The columns headed $\log E$ give the logarithms (to the base 10) of the intensities for different parts of the chromosphere. The intensities are expressed in ergs and refer to the emission per second in all directions from a slab of the chromosphere 1 cm thick, above the moon's edge and perpendicular to it. At the top of each column is given the mean height of the moon's edge above the solar limb for the exposure and the region in question. The subscripts 48 and 49 refer to two successive films of the series which were obtained near third contact. The columns headed $\log E_{49a}$ give the intensities aris-

² See Milne, *Handbuch der Astrophysik*, 3, Part I, 149, 1930.

³ *Verh. der Kon. Ak. van Wet.* (Amsterdam), 13, No. 5, 1928.

⁴ *Harvard Circ.*, No. 410, 1935.

⁵ *Lick Obs. Pub.*, 17, 1931.

ing from such a slab of the chromosphere when the moon's edge is 670 km beyond the limb of the sun; and the intensities, $\log E_{48a}$, refer to the same slab when the moon's edge is 1500 km beyond the sun's limb. This region appeared to be representative of the chromosphere as a whole, and we refer to it as normal. The column headed $\log E_{49b}$ refers to a region of the chromosphere where the excitation is abnormally high; the lines of hydrogen and especially of helium are very much enhanced.

3. THE CONTINUOUS BALMER EMISSION

This emission arises from the capture of free electrons in the second-quantum state. If $\frac{1}{2}mv^2$ is the kinetic energy of the electron before capture, the frequency of the emitted quantum is given by

$$h\nu = \frac{1}{2}mv^2 + \frac{hR}{4},$$

where

$$R = \frac{2\pi^2 m e^4}{h^3}.$$

The energy distribution in this spectrum depends upon the velocity distribution of the free electrons. If the latter is Maxwellian, corresponding to a temperature T , the energy emitted per second per cubic centimeter in a wave-number range, $d\tilde{\nu}$, of the continuum is

$$E_c d\tilde{\nu} = N_i N_e \frac{h^3}{(2\pi m k T)^{3/2}} \frac{2^4}{3\sqrt{3}\pi} \frac{8\pi^2 \epsilon^2 R^2}{m c^3} e^{(\chi_2 - h\nu)/kT} \frac{hc d\tilde{\nu}}{8}, \quad (3.1)$$

where N_i and N_e are the numbers of protons and electrons per cubic centimeter, respectively, and χ_2 is the ionization energy of hydrogen in the second quantum state.⁶ With numerical values equation (3.1) reduces to

$$E_c d\tilde{\nu} = [-22 \cdot 105] \frac{N_i N_e}{T^{3/2}} e^{(\chi_2 - h\nu)/kT} d\tilde{\nu}. \quad (3.2)$$

The energy distribution in this spectrum is therefore proportional to

$$e^{-h\nu/kT} d\tilde{\nu}. \quad (3.3)$$

⁶ Cillié, *M.N.*, **92**, 827, 1932.

The last row of Table 3 gives the intensities of the Balmer continuous spectrum for the three portions of the chromosphere at the respective wave-lengths λ 3640 and λ 3500. They express the emission in ergs per second over the complete solid angle and per unit wave-number of the continuum. Using equation (3.3), we find that T for the regions 49a and 49b is, respectively, $12,000^\circ$ and 9300° . These determinations are only approximate, because it is difficult to estimate accurately the intensity of the general emission of the chromosphere and the corona, on which the Balmer continuous spectrum is superposed. There is also the possibility of a systematic error in

TABLE 3
THE CONTINUOUS BALMER EMISSION

	UV 49a				UV 48a	UV 49b	
	3660	3647.4	3640	3500	3640	3640	3500
log B_{ac} (measured)	13.56	13.55	13.53	13.38	12.89	13.66	13.47
Correction for dispersion, etc.	1.38	1.38	1.38	1.36	1.38	1.38	1.36
log E_c (energy per unit wave-number)	12.18	12.17	12.15	12.02	11.51	12.28	12.11

our calibration. The determinations seem to indicate, however, that the electron temperature in the lower chromosphere is higher than the temperature usually associated with the radiation from the solar photosphere.

4. THE POPULATION OF THE EXCITED STATES OF HYDROGEN IN THE CHROMOSPHERE

Let N_{nT} be the number of hydrogen atoms in state n per cubic centimeter in an inclosure in thermodynamic equilibrium at temperature T . If the numbers of protons and electrons per cubic centimeter are N_i and N_e , then N_{nT} is given by

$$\frac{N_i N_e}{N_{nT}} = \frac{(2\pi m k T)^{3/2}}{h^3} \frac{1}{n^2} e^{-x_n/kT}. \quad (4.1)$$

If the actual number of chromospheric hydrogen atoms per cubic centimeter in state n is N_n , we introduce coefficients, b_n , defined by

$$b_n = \frac{N_n}{N_{nT}}. \quad (4.2)$$

It is the object of the present section to determine the observed values of b_n for the chromosphere.

The emission per cubic centimeter per second in the line H_n is

$$E_n = N_n A_{n2} h \nu_{n2}, \quad (4.3)$$

where A_{n2} is the Einstein coefficient of spontaneous transition, and ν_{n2} the frequency of the line. By equations (4.1), (4.2), and (4.3)

$$E_n = b_n N_i N_e \frac{h^3}{(2\pi m k T)^{3/2}} n^2 e^{x_n/kT} A_{n2} h \nu_{n2}. \quad (4.4)$$

From equations (3.1) and (4.4) we find

$$b_n = \frac{E_n}{E_c} \frac{2^4}{3\sqrt{3}\pi} \frac{8\pi^2 \epsilon^2 R^2}{m c^3} \frac{c}{8n^2 A_{n2} \nu_{n2}} e^{(x_2 - h\nu - x_n)/kT}. \quad (4.5)$$

At the Balmer limit $h\nu = x_2$, and introducing numerical values, we find

$$b_n = [8.992] \frac{E_n}{E_c} \frac{e^{-x_n/kT}}{n^2 A_{n2} \nu_{n2}}. \quad (4.6)$$

The observed values of E_n and E_c given in Tables 1, 2, and 3 refer to the emission of a large slab of the chromosphere and not to that of 1 cm.³. It is legitimate to use the ratio of the observed values only if the emission gradients of the lines H_n are the same as that for the continuum. But this condition is fulfilled only for the lines near the limit. The emission gradients of the lower members decrease as n decreases, probably on account of self-reversal. For these lines the values of b_n computed directly from the observed intensities are systematically too low.

In Table 4 values of $\log b_n$ computed by means of equation (4.6) are given for four different temperatures. The values of E_n/E_c refer

to the region 49a, and where the line has been observed on both series of films, *UV* and red, a mean is taken. The values of A_{n2} are those given by Menzel and Pekeris.⁷

By equation (4.6) we see that the value of b_n depends upon T through the factor $e^{-x_n/kT}$, which varies within wide limits when n is

TABLE 4
VALUES OF LOG b FOR DIFFERENT VALUES OF T

n	1000°	5000°	10,000°	20,000°
3.....	-7.08	-1.02	-0.26	+0.12
4.....	4.23	-0.82	-.40	-.18
5.....	3.01	-0.83	-.55	-.42
6.....	2.23	-0.71	-.42	-.32
7.....	1.73	-0.62	-.48	-.41
9.....	1.10	-0.43	-.34	-.30
10.....	1.03	-0.49	-.42	-.38
11.....	0.88	-0.43	-.38	-.35
12.....	0.66	-0.28	-.24	-.21
13.....	0.53	-0.21	-.17	-.15
14.....	0.48	-0.20	-.16	-.15
15.....	0.42	-0.18	-.15	-.14
16.....	0.37	-0.15	-.13	-.11
17.....	0.31	-0.12	-.09	-.08
18.....	0.30	-0.13	-.11	-.10
19.....	0.33	-0.18	-.16	-.15
20.....	0.21	-0.07	-.06	-.05
21.....	0.15	-0.02	-.01	.00
22.....	0.17	-0.06	-.04	-.04
23.....	0.10	+0.00	+.02	+.02
24.....	0.12	-0.02	.01	-.01
25.....	0.09	+0.00	+.01	+.01
26.....	0.05	+0.03	+.04	+.04
27.....	0.05	+0.02	+.03	+.04
28.....	0.03	+0.04	+.05	+.06
29.....	-0.05	+0.01	+.02	+.03
31.....	0.00	+0.06	+0.06	+0.07

small. When n is large, $e^{-x_n/kT}$ is close to unity for the temperature range under discussion. The values of b_n are therefore practically independent of T when n is large.

In Table 4 the numbers of excited hydrogen atoms in the chromosphere are compared with the numbers in an inclosure in thermodynamic equilibrium at different electron temperatures and containing the same numbers of ions and electrons. On the whole, there seems to be a deficiency of atoms in the lower and intermediate states.

⁷ *M.N.*, 96, 77, 1936.

When $20 < n < 32$, the populations of the states are very close to those for the thermodynamic inclosures. Since for these states b_n is approximately unity, we may write

$$N_n \sim N_{nT} \quad (4.7)$$

for $20 < n < 32$.

5. STATES FOR WHICH $n > 31$

Beyond H_{31} the members of the Balmer series overlap completely on the microphotometer tracings. The resulting continuous spectrum runs from $\lambda 3660$ to $\lambda 3647.4$, where it grades into the true Balmer continuum without any apparent discontinuity. From Table 3 it appears that the intensity in this spectrum for the region 49a is very nearly constant over the whole range. Using these observations, we deduce in the present section the values of b_n for the states for which $n > 31$.

Let the members of the Balmer series falling in a small wave-number range, $d\tilde{\nu}$, arise from transitions whose upper levels have quantum numbers in a range dn . Hence

$$d\tilde{\nu} = \frac{2R}{cn^3} dn. \quad (5.1)$$

If the intensity per unit wave-number in this spectrum is I ,

$$Id\tilde{\nu} = N_n dn A_{n2} h\nu_{n2}. \quad (5.2)$$

By equations (4.1) and (4.2)

$$N_n = b_n N_i N_e \frac{h^3}{(2\pi m k T)^{3/2}} n^2 e^{x_n/kT}. \quad (5.3)$$

According to Kramer's approximation⁸ for the Einstein transition coefficients,

$$A_{n2} = \frac{2^4}{3\sqrt{3}\pi} \frac{8\pi^2 \epsilon^2 R^2}{mc^3} \frac{1}{4n^5 \left(\frac{1}{4} - \frac{1}{n^2} \right)}. \quad (5.4)$$

⁸ *Ibid.*

Combining equations (5.2), (5.3), and (5.4), we find that

$$Id\tilde{\nu} = b_n N_i N_e \frac{h^3}{(2\pi m k T)^{3/2}} \frac{2^4}{3\sqrt{3}\pi} \frac{8\pi^2 \epsilon^2 R^2}{mc^3} \frac{ch}{8} e^{x_n/kT} d\tilde{\nu}. \quad (5.5)$$

We next compare the intensity in this spectrum with that in the true Balmer continuum. Divide equation (3.1) by equation (5.5) and

$$\frac{E_c}{I} = \frac{1}{b_n} e^{(\chi_2 - h\nu - x_n)/kT}.$$

If E_c refers to the Balmer continuum at the limit, $\chi_2 = h\nu$ and

$$b_n = \frac{I}{E_c} e^{-x_n/kT}.$$

For these high values of n , $e^{-x_n/kT} \sim 1$ and

$$b_n = \frac{I}{E_c}. \quad (5.6)$$

Since from Table 3 I is constant over this range and equal to E_c , b_n is unity in this range. Hence also for the states for which $n > 31$ we have

$$N_n = N_{nT}.$$

Owing to the action of near-by atoms and the radiation field, the states near the ionization limit will be broadened, and from a certain point they will overlap completely to form a continuum.⁹ In view of the finite resolving power of the instruments used, it is impossible to determine the point where this continuum begins. In this continuum the statement "number of atoms in state n " becomes meaningless, and the foregoing result has to be interpreted in a different way.

Let the number of atoms whose negative energies lie in the region between χ and $\chi + d\chi$ be $dN(\chi)$. Then by the foregoing,

$$dN(\chi) = N_{nT} dn,$$

⁹ Menzel, *Proc. Nat. Acad.*, **19**, 40, 1933.

where N_{nT} is given by equation (4.1) and dn is given by

$$d\chi = \frac{2hR}{n^3} dn.$$

It is also possible that, on account of the resolving power of the instruments, a deficiency of atoms with very small negative energies may not be detected on the tracing. Since H_{30} and H_{31} , which are less than 1 Å apart, are resolved on the tracing, and since a wavelength of 2 Å to the red of the Balmer limit corresponds to H_{85} , it is evident that such a deficiency occurs, if at all, only for energies corresponding to very high quantum numbers. From general physical principles it would appear that no discontinuity should arise.

6. THE POPULATION OF THE HIGHER STATES OF HYDROGEN IN A PURELY CAPTURE SPECTRUM

The theoretical emission decrement of the Balmer series has been discussed by various writers.¹⁰ The calculations have usually been based on the assumption that the spectrum is due purely to recombination. The condition of a steady state requires a balance between the number of atoms entering and the number of atoms leaving a given quantum level. A set of infinite simultaneous equations must be solved. Previous attacks on the problem have been concerned chiefly with the earlier members of the Balmer series. The higher equations were neglected. Such solutions give no information about the intensities of higher members of the series. We now proceed to outline a general method for solving the infinite determinant, by means of which the Balmer decrement can be computed to any desired degree of accuracy, by successive approximation. Further calculations are being made by Menzel and Baker, with the view of applying them to the planetary nebulae. For the purposes of the present section we shall adopt Kramers' approximation for the Einstein coefficients of spontaneous transition for hydrogen

$$A_{n''n} = \frac{2^4}{3\sqrt{3}} \frac{8\pi^2\epsilon^2 R^2}{\pi mc^3} \frac{2}{n''^5 n^3} \frac{1}{\frac{1}{n^2} - \frac{1}{n''^2}}, \quad (6.1)$$

¹⁰ H. H. Plaskett, *Harvard Circ.*, No. 335, 1928, and *Pub. Dom. Ap. Obs.*, **4**, 187, 1928; J. A. Carroll, *M.N.*, **90**, 588, 1930; Cillié, *ibid.*, **96**, 771, 1936.

which neglects the g -factor correction. Introduce

$$B = \frac{2^4}{3\sqrt{3}\pi} \frac{8\pi^2\epsilon^2 R^2}{mc^3}$$

and we may write

$$A_{n''n} = B \frac{2}{n''^5 n^3} \frac{1}{\frac{1}{n^2} - \frac{1}{n''^2}}. \quad (6.2)$$

Consider the equilibrium of state n in a purely capture spectrum. The number of atoms arriving in state n every second from higher states is

$$\sum_{n''=n+1}^{\infty} N_{n''} A_{n''n} = \frac{B}{n^3} \sum_{n''=n+1}^{\infty} \frac{2N_{n''}}{n''^5} \frac{1}{\frac{1}{n^2} - \frac{1}{n''^2}}.$$

Substituting for $N_{n''}$ from equation (5.3), this becomes

$$\sum_{n''=n+1}^{\infty} N_{n''} A_{n''n} = N_i N_e \frac{h^3}{(2\pi m k T)^{3/2}} \frac{B}{n^3} \sum_{n''=n+1}^{\infty} b_{n''} \frac{2}{n''^3} \frac{e^{\chi_{n''}/kT}}{\frac{1}{n^2} - \frac{1}{n''^2}}. \quad (6.3)$$

To obtain a solution of our problem we assume as a first approximation that the coefficients $b_{n''}$ change very slowly with n'' . We thus set $b_{n''} \sim b_n$ and remove it from the summation sign. Further remembering the definition of $\chi_{n''}$, we find for large n , to a high degree of approximation, that

$$\begin{aligned} \sum_{n''=n+1}^{\infty} \frac{2}{n''^3} \frac{e^{-(\chi_n - \chi_{n''})/kT}}{\frac{1}{n^2} - \frac{1}{n''^2}} &= \int_{(\chi_n - \chi_{n+1})/kT}^{\chi_n/kT} e^{-x} \frac{dx}{x} \\ &= Ei\left(\frac{\chi_n}{kT}\right) - Ei\left(-\frac{\chi_n - \chi_{n+1}}{kT}\right). \end{aligned}$$

When n is large, χ_n/kT and χ_{n+1}/kT are very small, and

$$-Ei\left(-\frac{\chi_n}{kT}\right) \sim -\gamma - \ln \frac{hR}{n^2 kT}, \quad (6.4)$$

where γ is Euler's constant, 0.5772. Introducing this approximation in the foregoing equation, we find

$$\sum_{n''=n+1}^{\infty} \frac{2}{n'^3} \frac{e^{-(x_n - x_{n''})/kT}}{\frac{1}{n^2} - \frac{1}{n'^2}} = \ln \left\{ \frac{(n+1)^2}{2n+1} \right\}.$$

Hence, from equation (6.3)

$$\sum_{n''=n+1}^{\infty} N_{n''} A_{n''n} = b_n N_i N_e \frac{h^3}{(2\pi m k T)^{3/2}} e^{x_n/kT} \frac{B}{n^3} \ln \left\{ \frac{(n+1)^2}{2n+1} \right\}. \quad (6.5)$$

Besides the mathematical approximations made in deriving equation (6.5), there is the further assumption that there are atoms in all quantum states, even when $n'' \rightarrow \infty$. In the previous section it was pointed out that one has to regard the states of very small negative energy not as discrete, but as forming a continuum. It appeared there that the distinction is a purely formal one.

The number of atoms arriving in state n per second by direct capture is

$$N_i N_e \frac{h^3}{(2\pi m k T)^{3/2}} \frac{B}{n^3} e^{x_n/kT} \left\{ -Ei \left(-\frac{x_n}{kT} \right) \right\}^{11}$$

With the approximation equation (6.4) this becomes

$$N_i N_e \frac{h^3}{(2\pi m k T)^{3/2}} \frac{B}{n^3} e^{x_n/kT} \left(-\gamma - \ln \frac{hR}{n^2 k T} \right). \quad (6.6)$$

The number leaving state n for lower states every second is

$$\sum_{n'=1}^{n-1} N_n A_{nn'} = N_n \frac{2B}{n^5} \sum_{n'=1}^{n-1} \frac{1}{n'^3} \frac{1}{\frac{1}{n'^2} - \frac{1}{n^2}}, \quad (6.7)$$

where we have used the approximation equation (6.2). Now

$$\sum_{n'=1}^{n-1} \frac{1}{n'^3} \frac{1}{\frac{1}{n'^2} - \frac{1}{n^2}} = 2 \sum_{n'=1}^{n-1} \frac{1}{n'} - \frac{1}{2} \sum_{n'=1}^{2n-1} \frac{1}{n'} + \frac{1}{2n}. \quad (6.8)$$

¹¹ *M.N.*, **92**, 823, 1932.

We further have that

$$\ln(m+1) + \gamma - \sum_{n'=1}^m \frac{1}{n'} < \frac{1}{2} \sum_{n'=1}^{\infty} \frac{1}{(m+n')^2}.$$

For large m , therefore, we may introduce the approximation

$$\sum_{n'=1}^m \frac{1}{n'} = \ln(m+1) + \gamma.$$

Introduce this equation in (6.8):

$$\sum_{n'=1}^{n-1} \frac{1}{n'^3} \frac{1}{\frac{1}{n'^2} - \frac{1}{n^2}} = \frac{1}{2} \{3\ln n + 3\gamma - \ln 2\}.$$

Substitute this equation in (6.7) and also the value of N_n from equation (5.3):

$$\sum_{n'=1}^{n-1} N_n A_{nn'} = b_n N_n N_e \frac{h^3}{(2\pi m k T)^{3/2}} e^{x_n/kT} \frac{B}{n^3} \{3\ln n + 3\gamma - \ln 2\}. \quad (6.9)$$

In a steady state the number of atoms arriving in state n is equal to the number leaving it. Hence, from equations (6.5), (6.6), and (6.9) we find

$$b_n \ln \left\{ \frac{(n+1)^2}{2n+1} \right\} - \gamma - \ln \frac{hR}{n^2 k T} = b_n \{3\ln n + 3\gamma - \ln 2\}.$$

We may now solve for b_n . With numerical values and for large n we obtain

$$b_n = \frac{2\ln n + \ln T - 12.55}{2\ln n + 1.732}. \quad (6.10)$$

The value of b_n changes very slowly with n , which is in accordance with the assumption made above in order to derive the first approximation. b_n is also not very sensitive to changes in T . For $T = 10,000^\circ$ and $n = 30$ we find $b_n = 0.406$. According to equation

(6.10), $b_n \rightarrow 1$ as $n \rightarrow \infty$. This behavior is in accord with expectations, because the real continuum of the hydrogen atom should grade into the continuum on the other side of the ionization limit without a discontinuity. With the aid of equations (6.3) and (6.10) we may now carry out successive approximations and calculate b_n to any desired degree of accuracy.

If the hydrogen has considerable optical thickness in the Lyman lines, there will be reabsorptions of these radiations. This process tends to increase the theoretical numbers of atoms in the excited states. For instance, if there is so much self-reversal in the Lyman lines that the number of atoms leaving state n per cubic centimeter for state 1 is equal to the number of excitations from state 1 to state n , we find that the net number of atoms leaving state n for lower states is

$$\sum_{n'=2}^{n-1} N_n A_{nn'}.$$

Introducing the same approximations as for equation (6.7), we find

$$\sum_{n'=2}^{n-1} N_n A_{nn'} = b_n N_i N_e \frac{h^3}{(2\pi m k T)^{3/2}} e^{x_n/kT} \frac{B}{n^3} [3 \ln n + 3\gamma - \ln 2 - 2].$$

Using this expression instead of equation (6.9) and solving for b_n as before, we obtain the result:

$$b_n = \frac{2 \ln n + \ln T - \gamma - \ln \frac{hR}{k}}{2 \ln n + 3\gamma - 2}. \quad (6.11)$$

For $T = 10,000^\circ$ and $n = 30$, this gives $b_n = 0.530$.

The observed values of b_n for the chromosphere are very close to unity when $n > 20$. Hence the numbers of atoms in the higher states of hydrogen in the chromosphere are more than double the numbers one would expect from a purely capture spectrum. If the spectrum arises from capture, and if there is complete reversal in the Lyman lines, the difference between theory and observation is still a factor of 2. In the chromosphere there is therefore a process (or processes), besides capture and reversal of the Lyman lines, that controls the

populations of these upper levels. The process that presents itself most naturally is line excitation of the chromospheric hydrogen by the photospheric radiation, and we are inclined to believe that the Lyman line excitation is the most important.

7. LINE EXCITATION IN THE CHROMOSPHERE

By equations (6.5), (6.6), and (6.9) the number of chromospheric atoms per cubic centimeter arriving in state n every second and not accounted for on the capture theory is

$$N_i N_e \frac{h^3}{(2\pi m k T)^{3/2}} e^{x_n/kT} \frac{B}{n^3} \left[b_n(2l n n + 3\gamma) - 2l n n - \ln T + \gamma + l n \frac{hR}{k} \right]. \quad (7.1)$$

In the present section we shall suppose that this is the number of line excitations of the hydrogen by the photospheric beam. Since by observation $b_n \sim 1$ when n is large, equation (7.1) may be written

$$N_i N_e \frac{h^3}{(2\pi m k T)^{3/2}} e^{x_n/kT} \frac{B}{n^3} \left[4\gamma + l n \frac{hR}{k} - \ln T \right]. \quad (7.2)$$

The number of excitations to state n depends, in general, upon the populations of the lower states and upon the intensity of the photospheric radiation in the various wave-lengths. The number of atoms in the normal state cannot be observed directly. The number in state 2 can be estimated only from careful observations of the emission gradients of the lower members of the Balmer series, which enable one to deduce the amount of self-reversal. In view of the uncertainty of our intensity scale for the lower Balmer members, the relative numbers of atoms in the lower-quantum states, from 3 upward, are only imperfectly known. It is therefore impossible to discover, with the data of the present paper, from which states this line excitation takes place.

We can, however, determine a maximum value for the number of normal atoms by supposing that all the excitations (7.2) occur from the normal state.

The number of Ly_n excitations per cubic centimeter per second is

$$W N_1 B_{1n} I_\nu, \quad (7.3)$$

where I_ν is the intensity of the photospheric radiation in the region of Ly_n , W the dilution factor, and B_{1n} the usual Einstein coefficient. Introduce a parameter T_1 defined by

$$I_\nu = \frac{2h\nu^3}{c^2} \frac{1}{e^{h\nu/kT_1} - 1}, \quad (7.4)$$

where ν refers to a frequency in the neighborhood of the Lyman limit. T_1 is the temperature that specifies the intensity of the radiation in that region. Substitute for B_{1n} in terms of A_{n1} in equation (7.3) and introduce equation (7.4), and we find for the number of Ly_n excitations per cubic centimeter per second approximately

$$WN_1 n^2 A_{n1} e^{-(x_1 - x_n)/kT_1}. \quad (7.5)$$

According to the foregoing hypothesis—namely, that Lyman line excitation is solely responsible for the additional arrivals in state n —the expressions (7.2) and (7.5) are equal. Hence

$$WN_1 n^2 A_{n1} e^{-(x_1 - x_n)/kT_1} = N_i N_e \frac{h^3}{(2\pi m k T)^{3/2}} e^{x_n/kT} \frac{B}{n^3} \left[4\gamma + \ln \frac{hR}{k} - \ln T \right]. \quad (7.6)$$

Since by observation

$$\frac{N_i N_e}{N_n} = \frac{(2\pi m k T)^{3/2}}{h^3} \frac{1}{n^2} e^{-x_n/kT},$$

for the chromosphere when n is large, equation (7.6) may be written

$$\frac{N_i}{N_n} n^2 e^{-(x_1 - x_n)/kT_1} = \frac{1}{W} \frac{B}{n^5 A_{n1}} \left[4\gamma + \ln \frac{hR}{k} - \ln T \right]. \quad (7.7)$$

In thermodynamic equilibrium at temperature T_1 , the left-hand side of equation (7.7) is unity. In the chromosphere there is departure from thermodynamic equilibrium, and equation (7.7) indicates the extent of this departure with respect to the relative numbers of atoms in states 1 and n on the foregoing hypothesis. The right-hand

side of equation (7.7) is not very sensitive to changes of the electron temperature T . Adopting $T = 10,000^\circ$, we find

$$\frac{N_1}{N_n} n^2 e^{-(x_1 - x_n)/kT_1} = \frac{3 \cdot 19}{W}. \quad (7.8)$$

If we assume that W is of the order of $\frac{1}{2}$, the ratio of the numbers of atoms in states 1 and n by equation (7.8) is about six times the ratio for an inclosure in thermodynamic equilibrium at temperature T_1 . Since in the chromosphere there may be excitations from subordinate levels as well as from the ground level, equation (7.8) gives a maximum value for the left-hand side. The intensity of the photospheric radiation in the far ultraviolet region is not known with certainty, hence it is not possible to estimate T_1 or to determine a maximum for the ratio N_1/N_n .

A value of $\frac{1}{2}$ for W is based on the assumption that the exciting Lyman radiation comes from only one hemisphere. The opacity in the Lyman lines, however, may be sufficient to result in the production of an appreciable downward radiation stream, in which case $W \rightarrow 1$, with a corresponding value of 3.19 for the right-hand side of equation (7.8). The customary procedure of setting $W = \frac{1}{2}$ for various problems of stellar atmospheres as, for example, in Pannekoek's application of the ionization formula is open to question.

The most significant point of the foregoing calculations is that the process acting to produce the luminosity of the chromosphere, and also of the prominences, cannot be one of pure ionization from the ground state and subsequent recombination. The argument appears to require ruling out, or at least modifying, the hypothesis that radiation in the extreme ultraviolet portion of the solar spectrum, well beyond the Lyman limit, is responsible for chromospheric excitation.

HARVARD COLLEGE OBSERVATORY
and
UNIVERSITY OF THE WITWATERSRAND

THE ILLUMINATION OF REFLECTION NEBULAE

L. G. HENYEV

ABSTRACT

The general theory of the illumination of reflection nebulae by stars is discussed. It is shown that as far as large particles contribute to the scattering of the starlight, an equation of transfer, similar to the corresponding equation in the theory of the absorption and emission of light or in the theory of the scattering of light by small particles, is applicable. In this way it is possible to take into account the energy which has been scattered more than once by the particles of the nebula.

The theory has been translated into graphical form, by presenting a series of curves which give the distribution of the surface brightness on the faces of several ideal nebulae. Various important features of these curves are pointed out. When a nebula is illuminated by a star in front of it, the intensity gradient from the center outward varies inversely as the distance of the star from the nebula. When the star is inside of the medium, the gradient is even more steep. In the case of a thin nebula illuminated from behind, the bright nebula appears ring shaped if the particles in the nebula are large. For a more opaque nebula this ring shape is blurred over by the light which has suffered more than one reflection in passing through the medium.

The curves are applied to a number of actual nebulae. It is shown that the asymmetry of the nebulae IC 1284, IC 1287, and possibly BD+8°933 can be ascribed to an inclination of the faces of these nebulae to the line of sight. From the shape of the bright nebulosity near CD-24°12684 it is deduced that this star is immersed in the material. That this is the case is ascertained independently from the reddish color of the star and the nebula and from the faintness of the star, which seems to be cut down by about 3 mag. The nebula near ρ Ophiuchi is discussed and it is found that the star is about a parsec in front of the material.

I

Investigations of diffuse nebulae have resolved themselves principally into two groups. One has been concerned with the primary source of the light-energy which comes to us from these objects. Owing to the efforts of a number of astronomers, today we feel confident that the source of this energy lies in stars which are in proximity to the nebulae and that the light from these stars either is reflected by the particles of the nebulae into space or is momentarily absorbed by atoms which eventually re-emit the energy. The other group of investigations has consisted of the collection of evidence concerning the actual process of the reflection or scattering of the star's light, and aimed thereby to discover the nature of the particles which do the scattering. It seems plausible, in the present state of our knowledge, to say that the largest part of the scattered light comes from particles of fairly large dimensions (large with respect to the wave-

length of light), and is produced by a process somewhat similar to diffuse reflection but with the possible presence of diffraction effects. Probably a small amount of light is scattered by small particles, selectively with respect to the color and to the plane of polarization of the incident light. We shall see that a certain amount of observational evidence indicated that these small particles may be numerous, but are inefficient scatterers as compared with their absorbing power. Studies of the distribution of light over the apparent disks of nebulae have been devoted to questions involved in one of these two groups; photometric observations for their own sake have been rare.¹ In this paper we shall be concerned with the principles involved in such an investigation, with the development of the general properties to be expected in an ideal reflection nebula, and with an application of these results, in a semi-qualitative manner, to the distribution of light over the apparent disks of several actual nebulae.

The theory of the illumination of a dust cloud by a point source has been formulated in considerable detail in a series of papers by Seeliger.² An account of these papers may be found in the article by Schoenberg in the *Handbuch der Astrophysik*.³

Seeliger considers the intensity of the light reflected by each particle in the direction of the observer. The amount of energy which we receive from such a particle depends on four factors: (1) the distance of the particle from the source; (2) the degree to which other particles weaken, by occultations, the light falling on our particle; (3) the phase angle under which the light is reflected; and (4) the weakening, by occultations, of the light coming to us from the particle. The surface brightness of the nebula at any point on its disk is then equal to the contribution, within unit solid angle, of all the particles in a column with unit cross-sectional area, and directed along the line of sight.

Seeliger does not consider the contribution to the energy which we receive by reflections of the light coming from other particles; that

¹ The work of Keenan (*Ap. J.*, **84**, 600, 1936) on NGC 7023 is the only one dealing with nebulae having continuous spectra.

² "Zur Theorie der Beleuchtung der grossen Planeten, etc.," *Abhandlungen der Bayer. Akad.*, **16**, 1887; "Theorie der Beleuchtung staubförmiger Massen, etc.," *ibid.*, **18**, 1893; "Ueber kosmische Staubmassen, etc.," *Sitzung. d. Akad. zu Muenchen*, **3**, 1901.

³ 2, 130 ff. and esp. 163 ff.

is to say, he neglects the energy which has suffered more than one reflection during the interval of time which elapses after it leaves the source and until it again escapes from the nebula. In certain cases the effect of multiple reflections is not negligible, and consequently in a complete general theory they must be considered. This is done in the next section. We assume that the scattered light in reflection nebulae comes from large particles. However, our general formulae remain correct for any type of scattering process, and it is only on page 119, where we introduce the Euler phase function, and again on page 121, where we begin to use the Lambert phase function, that the discussion becomes limited to the case of large particles. It would be relatively easy to use other phase functions (e.g., those derived by Blumer from the equations of Mie), but it seems best not to complicate the analysis and to carry through our computations for the Lambert phase function, which, of course, is correct only for large spherical particles having smooth surfaces. The success of Seeliger's work in explaining the rings of Saturn and the zodiacal light is sufficient justification for our procedure. While I have not succeeded in finding a nebula which would give a rigorous test of the phase function, the methods for such a test have been derived, and their application has been illustrated by means of a few examples.

II

In the derivation of the fundamental equations governing the illumination of dust clouds we use what might be called a "microscopic" viewpoint as contrasted with the macroscopic viewpoint used by Seeliger. By this we mean that we consider the change which a ray of light undergoes within a small element of volume.

Consider a point and a ray, having a certain direction, situated in the nebula. Let us take an element of volume in the shape of a cylinder whose height is small compared with the diameter of its base. Let this cylinder be placed as shown in Figure 1, so that its base is perpendicular to the ray at the point. Represent its thickness by ds and the area of its base by $d\sigma$, the latter quantity being taken large compared to the cross-sectional area of the particles.

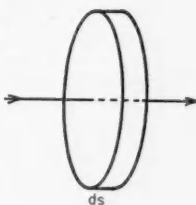


FIG. 1

The light coming in the direction of the ray and falling on the front surface of this element of volume is not uniformly distributed over the face. It may happen that particles, situated in front of the surface, are casting shadows on it, or that the same particles or others are reflecting light, coming from other directions, on it. Consequently, the illumination may vary from complete darkness to some maximum value. If the average value of the specific intensity over the surface is I , then the total energy falling on the face in unit time and in unit solid angle is given by

$$I d\sigma. \quad (1)$$

Before the light passes through the cylinder and falls on the back surface, part of its energy will be removed by falling on the particles in the volume. Take the average cross-sectional area of the particles to be $\pi\rho^2$, where ρ is the square root of the mean of the square of the radii. If the number of particles per unit volume is N , the total cross-sectional area exposed to the ray, in the element of volume, is

$$\pi\rho^2 N d\sigma ds.$$

Of course, it is possible that some of the particles are behind others and the total area is less than that stated, but if ds is chosen sufficiently small, the effect of such occultations over the distance ds is negligible. Not every fraction of this area is as effective as any other in absorbing light, since the illumination falling on $d\sigma$ is not uniform. Since we are interested only in average values, it is permissible to take $d\sigma$ sufficiently large so that, on the average, the irregularities cancel and we find that the light occulted by the particles is (per unit time and solid angle)

$$I \cdot \pi\rho^2 N d\sigma ds. \quad (2)$$

If the ray is inclined to the face of the cylinder, it is found that the amount of energy is given by the same formula.

In addition to the change in the intensity due to absorption, there is an increase due to the deflection of light from other directions into the one in which we are interested. We have seen that the

amount of energy absorbed from such an inclined ray is (per unit time and solid angle)

$$I' \cdot \pi \rho^2 N d\sigma ds,$$

where I' is its average intensity. A certain fraction of this energy is deflected in the direction of the first ray. This fraction depends on the directions of the two rays and on the kind of particles involved. We will denote it by Φ . Consequently, the energy deflected is

$$\pi \rho^2 N I' d\sigma ds \cdot \Phi.$$

The total contribution is this quantity summed over all directions, or

$$\pi \rho^2 N d\sigma ds \oint I' \Phi d\omega, \quad (3)$$

where the notation $\oint (\) d\omega$ represents the integral of the integrand over all solid angles.

Accordingly, the net gain in energy is

$$\pi \rho^2 N d\sigma ds \oint I' \Phi d\omega - \pi \rho^2 N I d\sigma ds. \quad (4)$$

If the specific intensity of the light falling on the back surface of our element of volume is $I + dI$, then, according to (1) and (4),

$$(I + dI)d\sigma - Id\sigma = \pi \rho^2 N d\sigma ds \oint I' \Phi d\omega - \pi \rho^2 N I d\sigma ds,$$

or, after some reduction,

$$\frac{1}{k} \frac{dI}{ds} + I = \oint I' \Phi d\omega, \quad (5)$$

where k , the absorption coefficient, is written for $\pi \rho^2 N$.

It will be seen that equation (5) is entirely similar to the corresponding relationship in the theory of absorption and emission of light or in the theory of scattering by small particles. Suppose that scattering particles are present in addition to reflecting particles. We must then replace (5) by the following equation:

$$\frac{1}{k_1 + k_2} \frac{dI}{ds} + I = \oint I' \frac{k_1 \Phi_1 + k_2 \Phi_2}{k_1 + k_2} d\omega, \quad (6)$$

where the subscript 1 refers to the reflecting particles and the subscript 2 refers to the scattering particles. The total absorption coefficient is therefore the sum of the individual absorption coefficients and the net phase function is the weighted mean of the individual phase functions. This statement holds for any admixture of any number of different kinds of particles.

The quantity Φ is, in the simplest case, a function only of the angle by which the light is deflected, or the phase angle, provided we refer to mean values. It is possible that, in some cases, it also depends on a second angle which determines the plane of the incident and of the reflected rays. What is most troublesome in this more general case is that the dependence of Φ on this second angle is not an explicit one, but involves other circumstances. For instance, if the rays have a definite amount of polarization, and if the reflecting or diffusing surfaces are such that the reflectivity depends on the plane of polarization of a plane-polarized ray, the reflection in a certain direction is different for the two polarized components of a partially polarized ray. The two components must be taken such that one is in the plane of the incident and reflected rays, and the other is perpendicular to it. The function Φ can then be conveniently replaced by two other functions, Φ_1 and Φ_2 , such that the first applies to one component and the latter to the other component. For mean values these functions depend only on the phase angle, except for preferentially oriented particles. It is necessary to specify additional quantities, defining the percentage of polarization and the position of the plane of maximum polarization, at each point in the medium and for every ray passing through the point.

Another property that the quantity Φ may have is that of depending on the wave-length. Most simply, the dependence on the phase angle may be the same for all colors, so that Φ is proportional to a certain function of this angle; in this case the constant of proportionality would depend on the wave-length. In any case one must investigate each color separately.

The dependence of the phase function on the phase angle may be extremely complicated, especially in the case of fairly large irregular

particles. When the diameters of the scattering particles are of the order of size of the wave-length of light, diffraction effects control, to a considerable extent, the nature of the phase function. Using the electromagnetic theory of light, Mie has investigated the process of scattering by small, spherical, and homogeneous particles, and among other important results has given various kinds of phase functions which depend on the size and the electromagnetic properties of the particles. For particles which are other than spherical the dependence is considerably different, but it is sufficiently well represented by the spherical case for qualitative purposes. An infinite variety of such functions is possible for different materials and sizes. This variety is lacking when one turns to larger particles: certain definite features are present when diffraction effects are negligible. The most important of these is the fact that no light is scattered forward in the direction of the incident light, since large opaque particles cast well-defined shadows in this direction. Although this is not a unique property of large particles, since in certain cases an approximately similar effect is present with small particles, the discovery of the effect in nebulae would be a strong point supporting the hypothesis of large particles. In a later paragraph I shall point out the conditions most favorable for observing this effect. At present definite evidence is not available for any known object in the sky.

With appropriate boundary conditions equation (5) serves in principle to determine the value of I at each point in space and for every direction. The boundary conditions consist of the values of I for each direction in space on a certain surface. Physically it is evident that this surface must be that at which a ray having a given direction enters the medium. This surface is then the outer boundary of the nebula, together with the surface of any stars which are imbedded in the nebula. The boundary conditions are consequently determined by the disposition of the external sources of illumination.

Formally, a solution of (5) is very easily obtainable. Let

$$I_0, I_1, I_2, \dots, I_i, \dots,$$

$$\left. \begin{aligned} &\frac{\mathfrak{I}}{k} \frac{dI_0}{ds} + I_0 = 0 \\ &\frac{\mathfrak{I}}{k} \frac{dI_i}{ds} + I_i = \oint I_{i-1} \Phi d\omega \\ &... .. \\ &\frac{\mathfrak{I}}{k} \frac{dI_i}{ds} + I_i = \oint I_{i-1} \Phi d\omega \\ &... .. \end{aligned} \right\} \quad (7)$$
$$I = I_0 + I_1 + I_2 + \dots + I_i + \dots \quad (8)$$
$$e^{\tau} I_i - I_{i0} = \int_0^{\tau} e^{\tau'} d\tau' \oint I_{i-1} \Phi d\omega,$$

or, since $I_{i0} = 0$ when $i > 0$,

$$I_i = \int_0^{\tau} e^{-(\tau-\tau')} d\tau' \oint I_{i-1} \Phi d\omega. \quad (9)$$

It is seen from these relations that I_0 represents the intensity of the light which has come directly from the sources and has passed through a portion of the medium. The quantity I_1 represents the intensity of the light which has been reflected once by the particles after leaving the sources, and correspondingly I_i represents that which has suffered i -reflections.

In most cases the source of illumination is a star, and it is more convenient to use the total intensity instead of the specific intensity, since a star is practically a point source. Therefore I_0 must be replaced by E , where

$$E = \frac{E_0}{r^2} e^{-\tau_0}, \quad (10)$$

where τ_0 is the optical distance from the entrance surface.

Using (10), we have for I_1

$$I_1 = \int_0^{\tau} e^{-(\tau-\tau')-\tau_0} \frac{E_0}{r^2} \Phi(\tau') d\tau', \quad (11)$$

where the quantities τ_0 , r , and Φ must be expressed in terms of τ . This equation is identical with the equation of Seeliger giving the intensity of the first-order reflected light.

The separation of I into component intensities may be the preferable method of solving certain problems, but in other cases the direct solution of the fundamental equation (5) may be more convenient.

III

Seeliger has computed the surface brightness of a uniform nebula, which is limited by parallel planes and which is illuminated by a distant source. It is convenient to have the specific intensity for every point and direction in the medium.

In Figure 2 let i be the angle of incidence of the light coming from the source. Then

$$E = \frac{E_0}{r^2} e^{-kz' \sec i}$$

for a point which is at a distance z' from the surface facing the star. Since the light from the source is approximately parallel, we have for the intensity in the direction of the arrow

$$I_1 = \frac{E_0}{r^2} \Phi \int_0^\tau e^{-(\tau - \tau') - kz' \sec i} d\tau'.$$

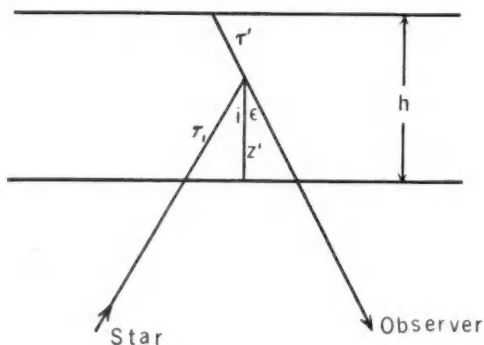


FIG. 2

Since the distance of the star from the nebula is large compared with the thickness of the nebula, the quantities r and Φ may be considered constant. When

$$0 < \epsilon < \frac{\pi}{2},$$

$$\tau' = k(h - z') \sec \epsilon, \quad \tau = k(h - z) \sec \epsilon,$$

and

$$\begin{aligned} I_1 &= \frac{E_0}{r^2} \Phi (i + \epsilon) k \sec \epsilon \int_z^h e^{-k(z' - z) \sec \epsilon - kz' \sec i} dz' \\ &= \frac{E_0}{r^2} \Phi (i + \epsilon) \frac{\sec \epsilon}{\sec i + \sec \epsilon} e^{kz \sec \epsilon} (e^{-kz(\sec \epsilon + \sec i)} - e^{-kh(\sec \epsilon + \sec i)}). \quad (12) \end{aligned}$$

When

$$\frac{\pi}{2} < \epsilon < \pi,$$

$$\tau' = -kz' \sec \epsilon, \quad \tau = -kz \sec \epsilon$$

and

$$\begin{aligned} I_1 &= -\frac{E_0}{r^2} \Phi(i + \epsilon) h \sec \epsilon \int_0^z e^{-k(z'-z) \sec \epsilon - kz' \sec \epsilon} i dz' \\ &= -\frac{E_0}{r^2} \Phi(i + \epsilon) \frac{\sec \epsilon}{\sec i + \sec \epsilon} e^{kz \sec \epsilon} \{1 - e^{-kh(\sec i + \sec \epsilon)}\}. \end{aligned} \quad (13)$$

The surface brightness on the side facing the star is obtained by substituting $z = 0$ in (12), that is,

$$I_1 = \frac{E_0}{r^2} \Phi(i + \epsilon) \frac{\sec \epsilon}{\sec i + \sec \epsilon} \{1 - e^{-kh(\sec i + \sec \epsilon)}\}.$$

The surface brightness on the other side is found from (13) by substituting $z = h$:

$$I_1 = -\frac{E_0}{r^2} \Phi(i + \epsilon) \frac{\sec \epsilon}{\sec i + \sec \epsilon} e^{kh \sec \epsilon} \{1 - e^{-kh(\sec i + \sec \epsilon)}\}.$$

As we have remarked, these relationships are valid when the source is sufficiently far from the nebula. This restriction need not be taken too seriously since the errors introduced by assumptions of uniformity may be more serious in actual applications.

In order to use these formulae we must be able to express r and i in terms of the apparent or angular distance of a point on the surface from the source. From Figure 3 we find that

$$\tan i = \frac{\delta}{x} \sec \epsilon - \tan \epsilon \quad \text{and} \quad r = x \sec i.$$

The results of equations (12) and (13) must be completed by the inclusion of the higher-order intensities. From the definition of these quantities we see that I_i is proportional to $(\mathcal{F} \Phi d\omega)^i$. Since this quantity, the albedo, is generally small, the higher-order intensities

approach zero. We will content ourselves with an examination of the order of size of I_2 , for a plane parallel nebula illuminated by a distant source, and neglect all other terms.

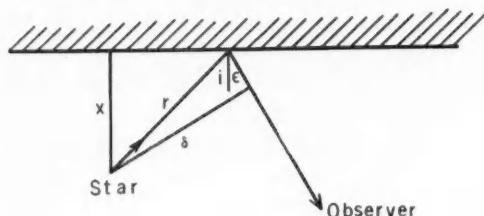


FIG. 3

From (9) we have

$$I_2 = \int_0^{\tau} e^{-(\tau-r')} d\tau' \mathcal{F} I_1 \Phi d\omega.$$

As before, we take (using ϕ as ϵ , as in Fig. 2):

$$\tau' = k(h - z') \sec \phi, \quad \tau = k(h - z) \sec \phi,$$

when

$$0 < \phi < \frac{\pi}{2},$$

and

$$\tau' = -kz' \sec \phi, \quad \tau = -kz \sec \phi,$$

when

$$\frac{\pi}{2} < \phi < \pi.$$

The quantity I_1 is given in equations (12) and (13), where z' must be substituted for z to avoid confusion. Let θ' be the angle between the projection on the face of the nebula of the original incident ray coming from the source, and the projection of the direction of I_1 . Also let θ be the corresponding angle for I_2 . Then

$$d\omega = \sin \epsilon \, d\epsilon d\theta'.$$

In the phase function we can no longer use $i + \epsilon$, since the third dimension is involved, and we introduce the angles α' and α , which

are, respectively, the supplements of the angles between I_0 and I_1 , and I_1 and I_2 . They are found from

$$\cos \alpha' = \cos i \cos \epsilon - \sin i \sin \epsilon \cos \theta',$$

and

$$\cos \alpha = -\cos \epsilon \cos \varphi - \sin \epsilon \sin \varphi \cos (\theta - \theta').$$

The phase function we will use is that of Euler:⁴

$$\Phi(\alpha) = \frac{\gamma}{4\pi} (1 + \cos \alpha).$$

We have for the emergent light, when $0 < \varphi < \pi/2$,

$$I_2 = k \sec \varphi \int_0^h \int_0^\pi \int_0^{2\pi} e^{-kz' \sec \varphi} \Phi(\alpha) I_1 \sin \epsilon \, d\theta' d\epsilon \, dz';$$

and when $\pi/2 < \phi < \pi$,

$$I_2 = -k \sec \varphi \int_0^h \int_0^\pi \int_0^{2\pi} e^{k(h-z') \sec \varphi} \Phi(\alpha) I_1 \sin \epsilon \, d\theta' d\epsilon \, dz'.$$

To get an estimate of the order of magnitude of the effect we shall simply consider the case when $i = 0$ and when $\phi = 0$ or 180° . Then, integrating for θ' ,

$$I_2 = 2\pi k e^{-kh} \int_0^h \int_0^\pi e^{kz' \sec \varphi} \Phi(\alpha) I_1 \sin \epsilon \, d\epsilon \, dz',$$

since the integrand is independent of θ' . Now

$$I_1 = \frac{E_0}{r^2} \Phi(\alpha') \frac{\sec \epsilon}{1 + \sec \epsilon} (e^{-kz'} - e^{-kh(1+\sec \epsilon)+kz' \sec \epsilon}),$$

when $0 < \epsilon < \pi/2$, and in the case when $\pi/2 < \epsilon < \pi$:

$$I_1 = -\frac{E_0}{r^2} \Phi(\alpha') \frac{\sec \epsilon}{1 + \sec \epsilon} (e^{kz' \sec \epsilon} - e^{-kz'}).$$

⁴ This phase function is adopted because of its simple form, and it bears a sufficient resemblance to the Lambert phase function to justify its use here. In general, the higher-order intensities are less sensitive to the shape of the phase function than is the first-order intensity.

Substituting and integrating for z' , we have

$$I_2 = 2\pi \frac{E_0}{r^2} e^{-kh} \left\{ \int_0^{\pi/2} \Phi(\alpha) \Phi(\alpha') \frac{\sin \epsilon}{1 + \cos \epsilon} \left[kh - \frac{1 - e^{-kh(1+\sec \epsilon)}}{1 + \sec \epsilon} \right] d\epsilon \right. \\ \left. - \int_{\pi/2}^{\pi} \Phi(\alpha) \Phi(\alpha') \frac{\sin \epsilon}{1 + \cos \epsilon} \left[\frac{e^{kh(1+\sec \epsilon)} - 1}{1 + \sec \epsilon} - kh \right] d\epsilon \right\};$$

or, if we put $p = kh$ and substitute for Φ :

$$I_2 = \frac{\gamma^2}{8\pi} \frac{E_0}{r^2} e^{-p} \left\{ \int_0^{\pi/2} (1 + \cos \epsilon) \sin \epsilon \left[p - \frac{1 - e^{-p(1+\sec \epsilon)}}{1 + \sec \epsilon} \right] d\epsilon \right. \\ \left. - \int_{\pi/2}^{\pi} (1 + \cos \epsilon) \sin \epsilon \left[\frac{e^{p(1+\sec \epsilon)} - 1}{1 + \sec \epsilon} - p \right] d\epsilon \right\}.$$

Now if we place $u = \sec \epsilon$ in the first integral and $u = -\sec \epsilon$ in the second one, we can reduce the expression to

$$I_2 = \frac{\gamma^2}{8\pi} \frac{E_0}{r^2} e^{-p} \left\{ \int_1^{\infty} \frac{1+u}{u^3} \left[p - \frac{1 - e^{-p(1+u)}}{1+u} \right] du \right. \\ \left. + \int_1^{\infty} \frac{u-1}{u^3} \left[p - \frac{1 - e^{-p(u-1)}}{u-1} \right] du \right\}.$$

Combining similar terms, we get

$$I_2 = \frac{\gamma^2}{8\pi} \frac{E_0}{r^2} e^{-p} \left\{ 2p \int_1^{\infty} \frac{du}{u^2} - 2 \int_1^{\infty} \frac{du}{u^3} + (e^{-p} + e^p) \int_1^{\infty} \frac{e^{-pu}}{u^3} du \right\}.$$

Also making use of the formula

$$\int_1^{\infty} \frac{e^{-qx}}{x^3} dx = \frac{1}{2} [e^{-q}(1-q) - q^2 Ei(-q)],$$

where $Ei(q)$ is the exponential integral function

$$\int_{-q}^{\infty} \frac{e^{-x}}{x} dx,$$

we arrive at the expression

$$I_2 = \frac{\gamma^2}{16\pi} \frac{E_0}{r^2} \left\{ e^{-p}(3p-1) - e^{-3p}(p-1) - p^2(e^{-2p}+1)Ei(-p) \right\}.$$

In a similar manner we can evaluate the case of $\varphi = 0^\circ$. For this the final result is

$$I_2 = \frac{\gamma^2 E_0}{8\pi r^2} \left\{ \frac{1 - e^{-2p}}{2} - pe^{-p} - p^2 e^{-p} Ei(-p) \right\}.$$

The values of the exponential integral function are available in the tables of Jahnke and Emde.⁵

The curves shown in Figure 4 represent the surface brightness of a thin nebula as a function of δ/x . In other words, the distance x , between the star and the nebula, has been chosen as the unit of distance. The first set of curves has been computed for various values of ϵ less than 90° , and the second for values greater than 90° . The angle ϵ is the inclination of the nebula with respect to the sky, values larger than 90° indicating that the star is behind the nebula. In the first set the nebula is taken to be completely opaque, while in the second it is taken to have an optical thickness of 1 mag. By the optical thickness in magnitudes we mean the value of the quantity

$$2.5 \cdot \log_{10} e \cdot kh.$$

In addition, Figure 4 contains a set of curves for the surface brightnesses of nebulae having the various optical thicknesses shown accompanying each of the curves for the cases $\epsilon = 0^\circ$ and $\epsilon = 180^\circ$. Only one half of each curve is given for $\epsilon = 180^\circ$; the other half is symmetrical with the first.

In all the cases mentioned in the preceding paragraph the intensities are expressed in terms of the intensity of the starlight at unit distance (the distance x), multiplied by the reduction factor, giving the absorption suffered by the starlight as observed from the earth. This reduction factor comes into consideration only when the star is behind the nebula. In all cases the intensities are given in magnitudes per square degree.

The Lambert phase function, which is proportional to

$$\frac{2}{3\pi^2} [\sin \theta + (\pi - \theta) \cos \theta],$$

⁵ *Funktionentafeln*, Leipzig, 1933.

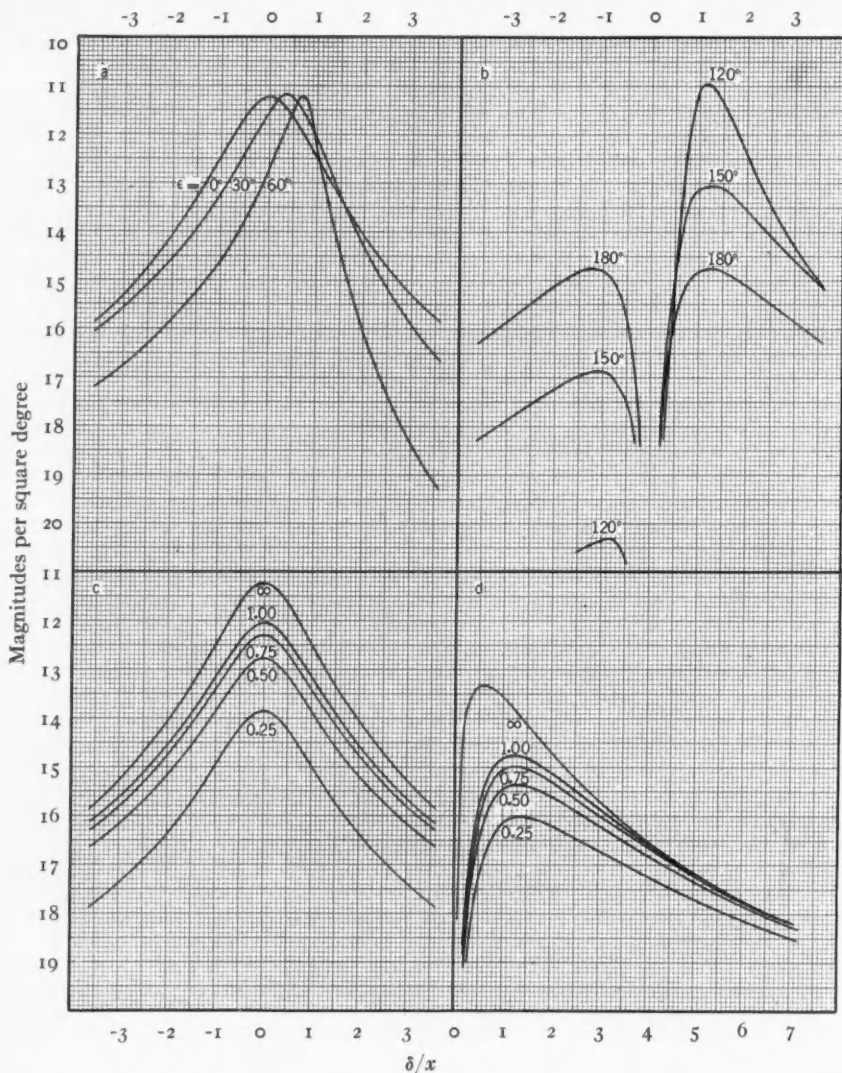


FIG. 4.—These curves display the distribution of brightness over a plane parallel nebula illuminated by a distant source. The albedo is taken to be unity. The Lambert phase function has been used. The unit of length is the perpendicular distance between star and nebula and the unit of intensity is the intensity of the star at this distance multiplied by the factor giving the obscuration of the star if the latter is seen through the nebula. The ordinates are given in magnitudes per square degree as referred to the unit, while the abscissa represents the quantity δ/x (see Fig. 3). (a) An infinitely opaque nebula observed on the same side as the star with the face inclined to the plane of the sky at the angles shown. (b) A nebula 1 mag. thick observed on the opposite side from the star and inclined at the angles shown. (c) Similar to (a), but for inclination zero and for various opacities as given in magnitudes. (d) Similar to (b), but for inclination zero and for various opacities.

has been used in computing the curves in Figure 4. This function is applicable to large spherical objects whose surfaces scatter light in proportion to the products of the cosines of the angles of incidence and of reflection. Whether such a function is applicable to the particles in a nebula is, of course, uncertain. Since no observational material is available on the actual nature of the nebular phase function, we need not hesitate to use one which satisfies the general conditions imposed by the theory of reflection by large particles. As has been stated previously, the most characteristic feature of the phase function for large particles is the condition

$$\Phi(\pi) = 0.$$

Its agreement with this condition and its mathematical simplicity are the reasons for the use of the Lambert phase function in this section, and for the use of the Euler function in the section on second-order reflections.

To find the brightness for a certain albedo γ , where

$$\gamma = \oint \Phi d\omega,$$

we must multiply each intensity by this quantity.⁶ This definition makes the albedo equal to the ratio of the total reflected light to the total incident light.

The surface brightness of a nebula which envelops its source was investigated by Seeliger, who derived an expression for the first-order intensity. The specific intensity in this case is

$$I_1 = \frac{2\gamma}{3\pi} \frac{E_0}{\delta^2} e^{\nu \cot \alpha_0} \{ \psi_\nu(\pi - \alpha_1) - \psi_\nu(\pi - \alpha_0) \},$$

where $\nu = k\delta$; the other quantities are explained in Figure 5. The function $\psi_\nu(\theta)$ has been computed by Seeliger for the Lambert phase function and is tabulated in his third paper, to which we have referred. He has used $\nu_1 = 0.4343\nu$ instead of ν . Knowing the shape of the nebula and the position of the star, one can evaluate the angles

⁶ This definition of the albedo is in many respects the most convenient one. Schoenberg uses another value which gives the specific intensity of the light reflected directly back by a single average particle.

α_0 and α_1 in terms of δ . These angles, together with the absorption coefficient, determine the values of $\psi_s(\theta)$.

The curves given in Figure 6a show the surface brightness as a function of δ , for the case of a plane parallel and uniform nebula which has an optical thickness of one magnitude. The various cases shown represent the results for different distances of the star from the front surface of the nebula, the number accompanying each curve giving the ratio of this distance to the thickness of the medium. The unit of length is the distance between the two faces of the nebula, and the unit of intensity is the intensity of the starlight at unit distance multiplied by the exponential factor, giving the effect of

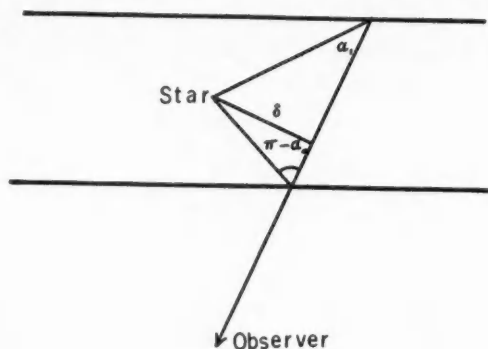


FIG. 5

the absorption along the line of sight. To reduce to a given albedo one must again multiply by γ . Figure 6b shows the same results in another form, the ordinates giving the intensities multiplied by the squares of the apparent distances, δ , between the star and the nebular points considered. Hence they represent the deviation from an inverse square law of intensity variation.

A similar set of curves is given in Figure 6c. The nebula is taken to be infinitely opaque, and the star is placed at the different optical depths given by the numbers, in magnitudes, accompanying each curve. In these cases the unit of length is the actual distance of the star from the front surface, and the unit of intensity is the actual intensity of the starlight at this surface, including the effect of absorption.

We have now to examine the importance of higher-order reflec-

tions. I have computed I_2 for two cases when the star is distant from the nebula: (a) $\varphi = 0^\circ$ and (b) $\varphi = 180^\circ$, both for a plane parallel nebula and for $i = 0^\circ$. The results are shown in Figures 7a and 7b for various values of the optical thickness of the nebula.

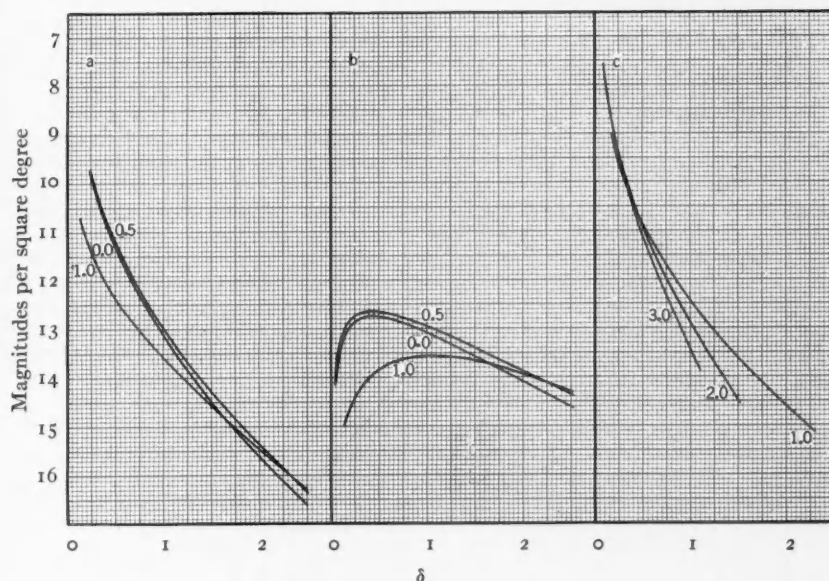


FIG. 6.—A plane parallel nebula internally illuminated. The unit of length is the distance between the faces and the unit of intensity is the star intensity at unit distance multiplied by the factor giving the absorption along the line of sight. The albedo is unity and the phase function which has been used is the Lambert. (a) The distribution for a nebula 1 mag. thick with the star placed at the various optical depths given in magnitudes. (b) Same as (a) but showing the deviation from an inverse square law of variation. (c) An infinitely opaque nebula with the star placed at the various optical depths shown. Here the unit of length is the actual distance of the star from the front face.

For an albedo γ the intensities must be multiplied by γ^2 . The relative importance of the second-order effect compared with the first will be proportional to γ . When $\epsilon = 0^\circ$ and $p \rightarrow \infty$, the maximum value of I_1 will correspond to 11.2 mag. per square degree (from Fig. 4c). The corresponding intensity I_2 will be 13.0 mag. per square degree. The difference in magnitude will give the ratio I_2/I_1 , for a certain value of γ :

$$0.19\gamma.$$

For any reasonable value of γ ($\frac{1}{3}$ or less) it will be seen that I_2 may be neglected.

When the star is behind the nebula, the situation is entirely different. Using as the value of the albedo $\frac{1}{5}$, we find for a nebula having an optical thickness of 0.75 mag. that I_2 corresponds to about 16.7 mag. per square degree. The maximum of I_1 is for x equal to

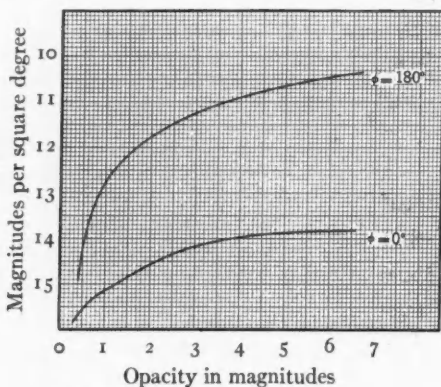


FIG. 7.—The second-order intensity for a plane parallel nebula. The albedo is taken to be unity. The phase function is the Euler. The units of length and intensity are the same as in Fig. 4. The intensity is shown for a point at the foot of the perpendicular from the star to the nebula and for the direction at right angles to the face. The intensity is shown for various opacities of the nebula.

$\phi = 0^\circ$ —the star in front of nebula
 $\phi = 180^\circ$ —the star behind nebula

about 1, and it corresponds to 16.8 mag. per square degree. The two intensities are nearly the same, while for denser nebulae I_2 increases rapidly with increasing optical thickness, and becomes much more important than I_1 . While no computations have been made for the third-order intensity, it is probable that this, too, would be large.

IV

The curves in Figures 4–6 display a number of features which, though depending on the simplifying assumptions we have made, are applicable in a qualitative way to actual nebulae. These as-

sumptions are: (1) the geometrical and physical uniformity of the nebula and (2) the applicability of the Lambert phase function.

Consider the case when the face of the nebula is perpendicular to the line of sight. When the star is in front of the nebula, the surface brightness near the projection of the star on the disk has a flat-topped maximum. If we now consider a position of the star nearer to the nebula, the surface brightness at each point increases. Since the curves in Figure 4 are drawn with the unit of length chosen equal to the distance between the star and the nebula, we shall see

that, as the star approaches the nebula, these curves must be compressed in the direction of the abscissae. It will be seen that not only does the surface brightness increase but the curve representing it becomes steeper. For a position of the star on the front surface (see Fig. 6) the surface brightness is very great near the star and decreases very rapidly with increasing distance. Near the star the intensity varies as $1/\delta$.

For positions of the star farther into the nebula the distribution of intensity is similar, as we see from Figure 6. As the star approaches the back surface of the nebula, the distribution of the surface intensity near the star becomes gradually steeper, but when it assumes a position just outside the nebula the central intensity has a minimum value. Higher-order reflections will tend to fill in this minimum and will somewhat modify the conclusions. The surface intensity increases with increasing distance from the star and, after reaching a maximum, decreases again (see Fig. 4). For positions of the star farther away, the central minimum is broader and the maxima are farther apart. If the second-order intensity is extremely strong, no minimum may be observed.

It must be emphasized that the small central intensity which we predict for thin nebulae depends to a certain extent on the phase function we have chosen. We have assumed that the type of scattering which is most common is that of diffuse reflection by large particles, for which

$$\Phi(\pi) = 0.$$

There are processes of scattering which do not satisfy this condition, but they involve particles which are of the same order of size as, or smaller than, the wave-length of light. As has been pointed out previously, observational evidence definitely favors the view that the particles are large. However, in all the cases considered, it is simple to replace the Lambert phase function by any appropriate phase function in order to satisfy the conditions of a problem. In general, very little change will be produced in the shape of any of the curves, except Figure 4*d*, by such a substitution, unless the new phase function is such that $\Phi(0)$ approaches zero. This is the case when the scattering particles are extremely small and scatter the light for-

ward instead of reflecting it back as in the case of large particles. Even then the intensity distribution over a nebula which is internally illuminated will not be affected greatly. But if the stellar source is outside of the medium, the situation is different. In the more important case of the star situated in front of the material, the first-order intensity may no longer be the largest part of the total intensity. It is obvious that a different treatment of the problem is needed. This problem is at present being investigated by the writer and will be discussed in a new paper.

An interesting feature of the curves is the asymmetry of the intensity distribution when a nebula is observed at an angle. The most important point which presents itself is the shift of the maximum surface brightness, depending on the inclination, when the star is in front of the nebula. These general features are independent of the phase function adopted. They are a result of the intensity distribution of the starlight falling on the nebula.

V

In this section we shall apply the curves, which have been given above, to some actual nebulae. In most cases no accurate photometric data are available, so that our conclusions will be of a preliminary character. Even when accurate observations are available, care must be exercised in applying the theory, since structural irregularities always distort and mask the general features which have been discussed. Actual galactic nebulae are certainly not the ideal objects which we have theoretically considered.

With accurate observations a great deal of information may be derived. In the first place, it is possible to ascertain whether the source is or is not within the boundaries of the nebular material. If it is inside or on the farther side, a knowledge of its distance, luminosity, and apparent brightness will determine the optical thickness of the material in front of it.

Furthermore, when the star is in the foreground, its distance from the front surface of the nebula may be determined in terms of the extent of the nebula or, if the parallax is known, in absolute units. This quantity may be found with reasonable certainty, since the shape of the intensity profile as given in any of the sets of curves

(Fig. 4) is remarkably similar for varying thicknesses of the medium. The procedure is simply to fit the scale along the abscissa to the observed case, and, since the unit of length is the quantity sought, it will be determined. If the star is immersed in a very opaque nebula, one can, if the obscuration of the star is known, get its true distance from the front surface in an analogous manner. When the star is in a thin layer of material, the true thickness of the layer may be determined from the optical thickness. In these two cases the absorption coefficient is given by the ratio of the optical distance to the true distance.

When a star is in front of a nebula with its surface inclined to the line of sight, an estimate can be made of this inclination. This may best be done by first considering the intensity distribution along a line perpendicular to the axis of symmetry and passing through the star. We can determine from this distribution the distance, in relative or absolute units, between the star and the point on the nebula immediately behind it. This distance is

$$x \csc \epsilon .$$

The distance to the point of maximum intensity is, in the same units, approximately

$$x \sin \epsilon .$$

From these two numbers ϵ may be computed.

One more important quantity is derivable from photometric data, namely, the albedo. Once the scale of the object has been determined, it is possible, in most cases, to derive this quantity from the relative brightness of the star and the nebula.

VI

Plates I and II reproduce photographs of reflection nebulae, which I shall discuss in detail. These are copied from plates taken by Professor E. E. Barnard and used in his *Atlas of Selected Regions of the Milky Way*.

The nebula IC 1287 falls in a region of fairly uniform dark nebulosity. It can be seen that the nebulosity is, nevertheless, one-sided, and the maximum intensity seems to be southwest of the star. The

nebula IC 1284 shows a similar characteristic; it extends farther toward the south in a field of uniform dark material. It seems highly probable that the face of the nebula in each case is inclined slightly to the line of sight and produces the observed effect. The stars would have to lie in front of the material, and this seems reasonable since the intensity gradient is, in both cases, very flat.

Indeed, we should expect to observe the majority of nebulae at an angle, since the probability of occurrence of a given ϵ is $\sin \epsilon$. The fact that most reflection nebulae are nearly or approximately symmetrical indicates that the stars illuminating the matter are generally near or actually inside of the nebula.

I have measured roughly the distance from the center of the nebula IC 1287 to the star and have found that $x \sin \epsilon$ is about $200''$. The width of the nebula perpendicular to the line joining the center and the star is around $750''$. Let us assume, for the sake of illustrating the method of analysis, that this distance is roughly $1.5x \csc \epsilon$. Then

$$x \sin \epsilon = 200'',$$

$$x \csc \epsilon = 500''.$$

We get from these relationships, very roughly, that

$$\epsilon = 35^\circ$$

and

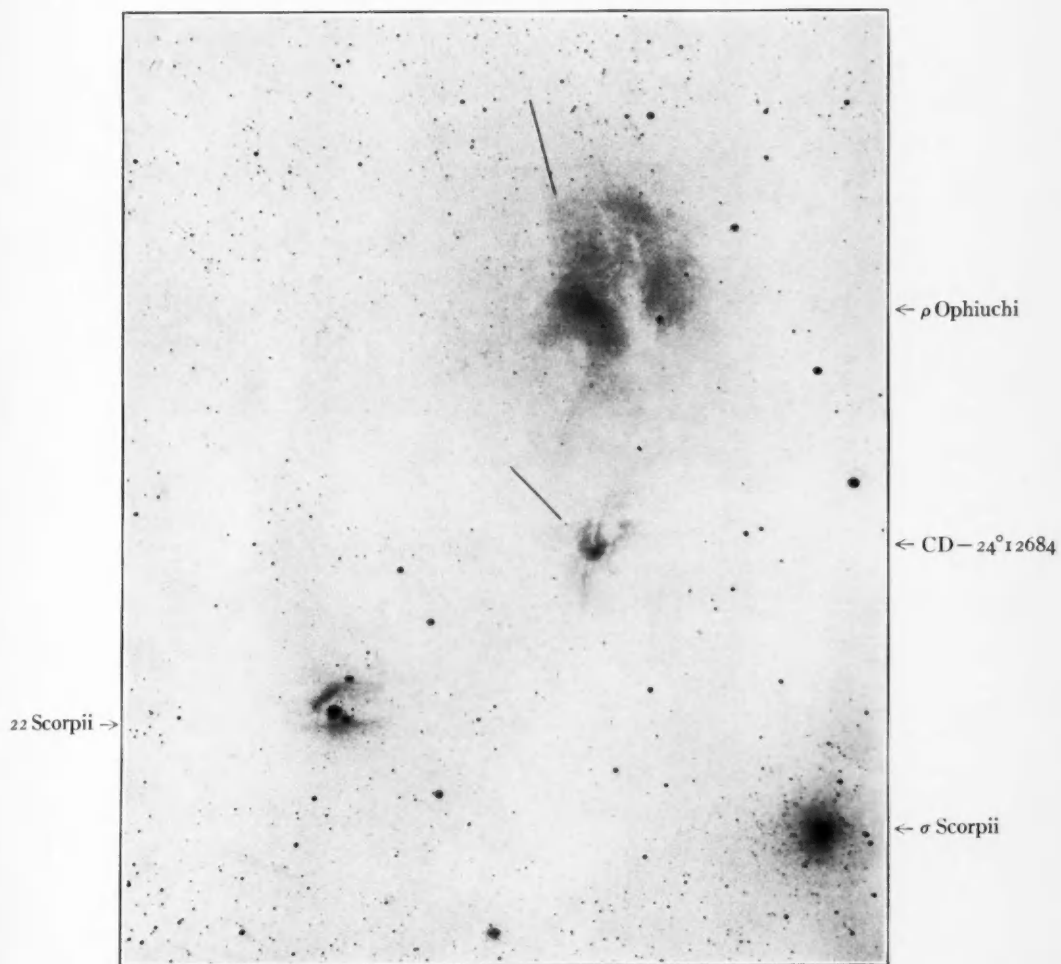
$$x = 300''.$$

From the spectral type, B₃, of BD-10°4713 I have estimated the distance of the star and nebula to be about 300 parsec. This gives

$$x = 100,000 \text{ astronomical units.}$$

Taking the absolute magnitude of a B₃ star as -1.0 mag., the apparent magnitude of the star at the nebula may be estimated at -7.5 . With an albedo of about $\frac{1}{4}$, the curve for 30° in Figure 4 gives as the surface brightness of the center of the nebula 5 mag. per square degree, which is half a magnitude fainter than the sky. These derived quantities are admittedly very rough, but their reasonableness is unquestionable and leads to the conclusion that the assumptions are consistent.

PLATE I



NEBULAE IN SCORPIUS AND OPHIUCHUS

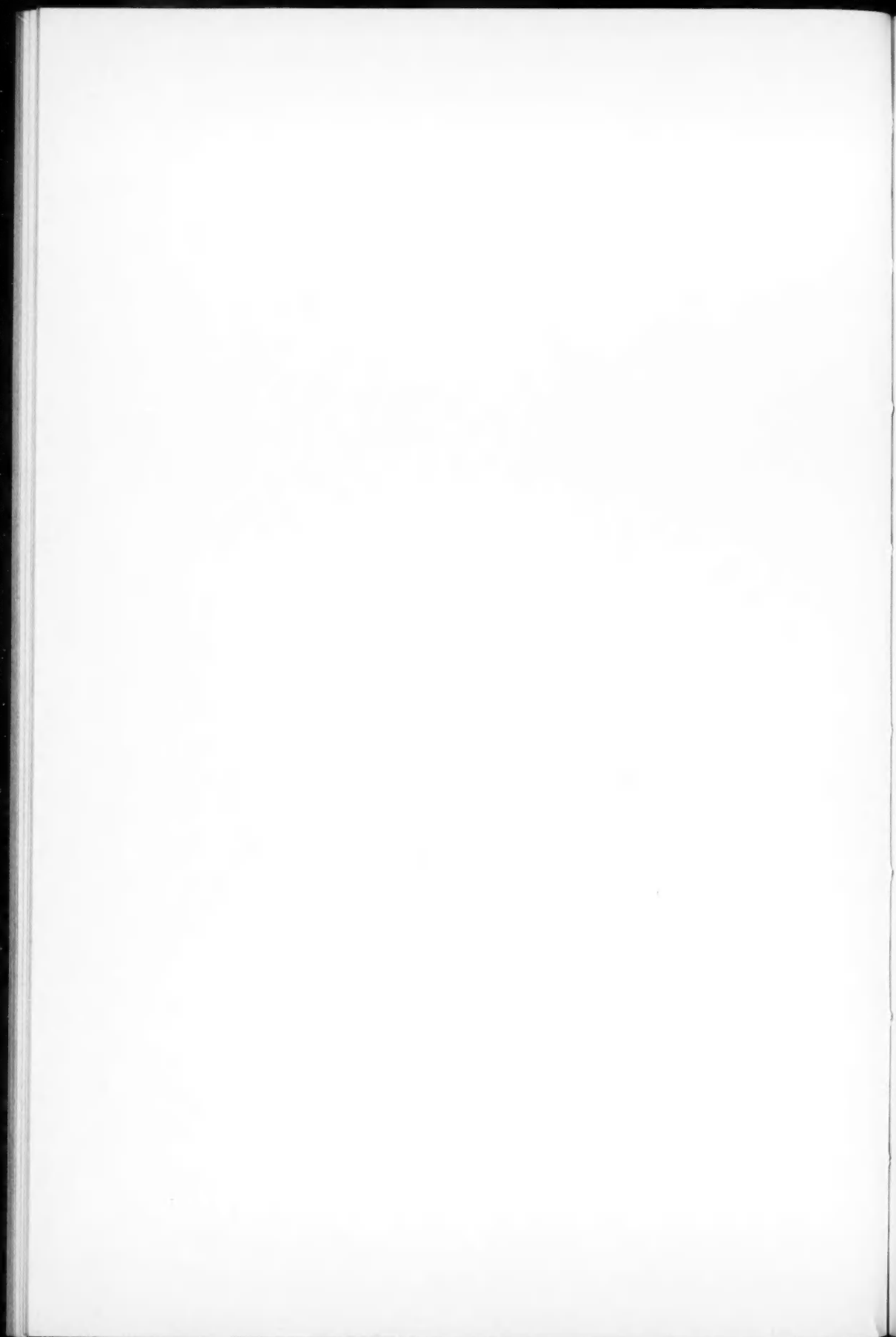
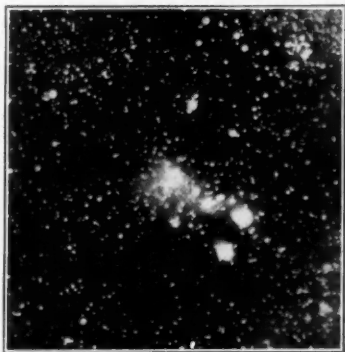


PLATE II



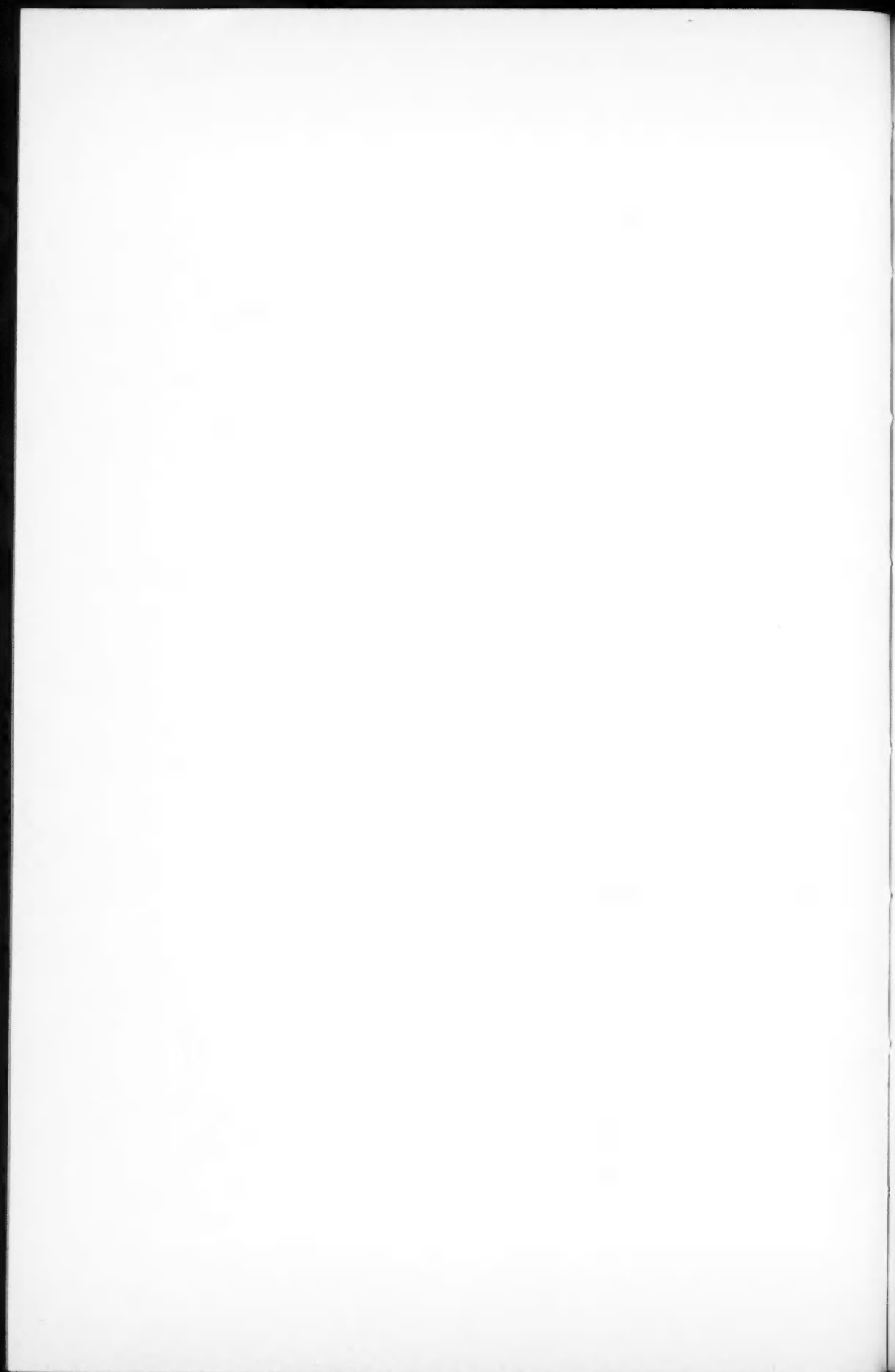
IC 1284



IC 1287



BD+8°933



The nebula around BD+8°933 is completely one-sided. There is dark material all around the star which is apparently connected with the bright patch. Since the material is almost completely dark next to the star, the latter cannot be immersed in it. It seems, then, that the nebula apparently near the star is in reality farther away, and we have possibly an extreme case of inclination. According to the curves in Figure 4a we should expect the intensity gradient to be smaller on the side of the maximum near the star. Since this is not the case, the distribution of the material must play a very important part in producing the fanlike shape of the bright nebula.

The group of nebulae in Scorpius and Ophiuchus, which are related to the extensive dark cloud in this region, contains some of the most interesting of these objects in the sky. The nebula which surrounds 22 Scorpii does so in a most peculiar manner. At first glance one is tempted to consider this system as a case of a star shining through a layer of nebulous matter. Indeed, some of the evidence points strongly toward such a hypothesis. The obscuring matter, which elsewhere is both dark and illuminated, extends right up to the star, and it is obvious that it is a part of the same cloud. This material, though not so dense as it is farther east, where it is practically opaque, seems to be fairly continuous. If it is behind the star, we should expect it to be uniformly illuminated. Very probably the particles are fairly large, since no evidence of selective scattering was found around ρ Ophiuchi and α Scorpii and no evidence of strong polarization was found around the former.⁷ The nebulae around these stars are connected continuously with one another and with that around 22 Scorpii. With large particles it is unlikely that the phase function is small for small phase angles. The lack of illumination near the star indicates that this matter must be in front of it. Since it is evident that very little second-order intensity is present, the albedo of the particles must be very small.

If we assume that this is indeed the case, we can estimate a lower limit for the absorption of the cloud. The distance from the bright ring to the star is about 250". Taking the distance of the system to be 100 parsec, the radius of the ring is 25,000 astronomical units. According to the curves for $\epsilon = 180^\circ$, this distance is slightly larger than the distance between the star and the nebula. We can say then

⁷ Struve, Elvey, and Roach, *Ap. J.*, **84**, 219, 1936.

that this latter distance is about 20,000 astronomical units, which gives as the apparent magnitude of 22 Scorpii, as seen from the nebula (taking $m = 4.9$),

$$4.9 - 5 \log \frac{100 \times 200,000}{20,000} = -10.1 \text{ mag.}$$

The maximum brightness of the nebula plus the sky is around 0.6 mag. brighter than the sky, making the nebula alone about 0.3 mag. fainter. Taking the brightness of the sky as 4.5 mag. per square degree, we have as the brightness of the nebula 4.8 mag. per square degree. For a given albedo we may find from these quantities the difference between star and nebula, or

$$4.8 + 2.5 \log \gamma + 10.1 = 14.9 + 2.5 \log \gamma.$$

Now, the albedo is, as we have said, very small. According to Figure 4*d*, we must then assume the nebula to be very opaque. For example, if $\gamma = 0.1$ (which is unreasonably large in view of the absence of the second-order intensity), the difference between star and

TABLE 1

STAR	SPECTRUM		MAG.	M	$m-M$	SEARES AND HUBBLE		INT. C.E.
	HD	Mt. W.				Sp.	C.E.	
β Scorpii.....	B1	Bon	2.90	-3.1	6.0			
σ Scorpii.....	B1		3.08	2.4	5.5	B1	+1.2	+0.5
ν Scorpii.....	B3	B2n	4.29	1.5	5.8			
CD-24°12684..	B3		8.0	0.9	8.9	B5	1.8	0.7
22 Scorpii.....	B3	B3n	4.87	0.9	5.8	B5	0.2	0.1
ρ Ophiuchi.....	B5	B4n	5.22	-0.6	5.8	B5	+1.1	+0.4

nebula becomes 12.4 mag. This is considerably above the maximum value of the ordinates in Figure 4*d*, corresponding to a completely opaque nebula. However, the star 22 Scorpii, which would necessarily suffer considerable obscuration according to these assumptions, cannot be cut down more than a few tenths of a magnitude. We see this from Table 1, in which are tabulated a number of stars, includ-

ing 22 Scorpii, all lying at approximately the same distance from us. Also tabulated are the spectra, the apparent magnitudes, the mean absolute magnitudes corresponding to the given spectrum,⁸ and the distance moduli. The last three columns give the spectral type and color excess according to Seares and Hubble⁹ and their color excess reduced to the International System. These distance moduli should be the same for each of the stars unless they are affected by absorption. Except for one star, to which we shall refer later, they are indeed the same.

It appears, then, that on the basis of our assumption concerning 22 Scorpii and its companion nebula, and on the basis of the principles discussed in this paper, we are led to a contradiction in the interpretation of the facts. It appears quite certain that 22 Scorpii is in front of its nebula.

Another object of considerable interest is the nebulous star CD-24°12684. The rapid decrease in the surface brightness of its nebula with increasing distance from the star suggests that we have here an example of a star imbedded in the material which it illuminates. To demonstrate this, density measurements on the original Bruce plates of Barnard were made along the lines shown in Plate II, for this object and for comparison for the nebula associated with ρ Ophiuchi. These are shown, as galvanometer deflections, in Figure 8, and they demonstrate the very rapid decrease in brightness in the former as compared with the very gradual falling-off in the latter object. The density near the stars is equal in the two cases, according to the curves, but an examination of Plate II reveals that there are a number of points near CD-24°12684 that are actually blacker than any near ρ Ophiuchi.

Two checks are available for testing independently the hypothesis of immersion. The comparison, in Table 1, of the spectral class, B₃, and the apparent magnitude of CD-24°12684 with that of other B-type stars in the vicinity of the dark nebula indicates that it is about 3 mag. fainter than it should be. This weakening is what would be expected from the absorption of the material in front of the star. In a private communication Miss Cannon states that she

⁸ Adams and Joy, *Mt. W. Contr.*, No. 244; *Ap. J.*, 56, 242, 1922.

⁹ *Ap. J.*, 52, 14, 1920.

has re-examined the spectrum of this star and has found that the *He* lines are very well marked, precluding the possibility of a spectrum of later type. Consequently, any doubt about the dependability of the comparison in this table would come from the dispersion in absolute magnitude, although it must be admitted that a deviation of 3 mag. is rare. That some of the other stars in the table are not of high luminosity was ascertained by an examination of a num-

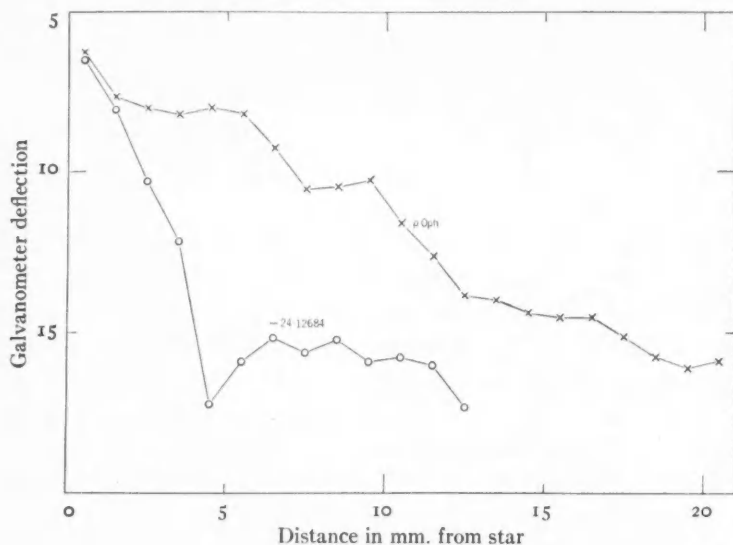


FIG. 8

ber of Yerkes spectrograms. No giant characteristics were found for β , σ , and ν Scorpii and for ρ Ophiuchi.

A second check is found in the color of the nebulosity. Two plates, one photographic and the other photovisual, which were taken with a Schmidt camera by Struve, Elvey, and Roach for their study of this region of nebulosity, were examined for color effects. It was found that, while the very bright filaments around ν Scorpii were almost absent on the photovisual plate, the nebulosity in question was quite bright. Measurements with a recording microphotometer verified this observation and showed that there exists a difference in color index between these nebulae of about 0.2 mag. No correction was made for the color of the sky and the color of the diffuse illumi-

nation emanating from Antares, which is south of 22 Scorpii and strongly illuminates the nebulosity around this latter star in long wave-lengths.¹⁰ Corrections for these effects are uncertain and would merely increase the difference found; therefore none was applied. The redness of the nebula CD-24°12684 may be explained by the fact that the source is shining through thick layers of nebulosity. This conclusion is verified in the most unexpected manner by the large color excess of -24°12684, as found by Seares and Hubble. The small value of the color excess for 22 Scorpii also agrees with our conclusions. That for ρ Ophiuchi is approximately one-half of that for -24°12684. It is extremely desirable that these color excesses be redetermined with greater accuracy.

Assuming that ρ Ophiuchi is in front of the nebula, I have computed its distance from the front surface. The brightness at a point about 30' north of ρ Ophiuchi is the same as that around Antares. Using the measures of Struve, Elvey, and Roach,¹¹ I find that this is 0.7 mag. fainter than the nebulosity immediately around ρ Ophiuchi. From the upper curve in Figure 4c this point is distant from the star by 0.7x. Taking the parallax of the star as 0".01, we get, approximately,

$$x = 250,000 \text{ astronomical units.}$$

For an absolute magnitude of -0.6 the apparent magnitude of the star at the nebula is -6.0. The brightness of the nebula, from the curve already used, is

$$11.2 - 6.0 - 2.5 \log \gamma.$$

¹⁰ The strong red light coming from Antares and scattered by the nebula makes the total red light around 22 Scorpii equal to that around CD-24°12684. This explains why no effect of reddening was detected by Struve, Elvey, and Roach in their original measurements on these plates. The measurements given in their Table 1 are substantially correct and do not conflict with the statements made in this paper. In fact, Struve states that he has visually found the nebula near 22 Scorpii to be bluer than the one near -24°12684.

¹¹ *Op. cit.*, Table 1. The references I make to these measures refer to their values corrected for the intensity of the sky.

From the measures of Struve, Elvey, and Roach this must be 1.2 mag. fainter than the sky, or about 5.7 mag. Equating and solving for γ , we find

$$\gamma = 0.6.$$

The measurements of CD - 24° 12684 have been fitted to the curve in Figure 6 for an optical depth of the source of 3 mag. Although no photometric standardization is available for any of the plates of Barnard, and although the measures were very rough, it is interesting to see what is obtained by assuming a linear relationship between intensity and galvanometer deflection. A fairly satisfactory fit was found when the distance of the star beyond the front surface was taken as 100,000 astronomical units, or 0.5 parsec. This result is interesting because it gives an approximate lower limit to the thickness of the nebula. In comparison with this, the diameter of the main central part of the dark nebula in Scorpius and Ophiuchus, not counting the arms, is about 5 parsec. Using this distance, we can compute another interesting quantity, the absorption coefficient, by dividing the absorption in the starlight by the distance just found; doing this, we get

$$k = 6 \text{ mag./parsec.}$$

This marked difference in the intensity distributions of the nebulosities we have discussed shows that Hubble's statistical method¹² cannot be applied to individual objects. For instance, the limiting diameter of the nebula associated with CD - 24° 12684 will behave differently, with varying exposure time, than will the diameter of a nebula for which the source is well outside of the medium.¹³ Otherwise, the results derived in this paper are in good agreement with those obtained by Struve and Story from an application of Hubble's method.

VII

The color excess of CD - 24° 12684, if interpreted as a result of Rayleigh scattering, would lead to a total photographic absorption

¹² *Mt. W. Contr.*, No. 250; *Ap. J.*, 56, 1922.

¹³ However, diffuse reflection nebulae with the source inside are apparently rare, because of the large coefficient of absorption of nebular material, which causes both star and nebula to appear faint.

by small particles of the order of 1 mag. Since the observed absorption is at least 3 mag., we could attribute the remaining absorption of 2 mag. to large particles. It would be premature, however, to consider this result as final. Our observations have failed to give us a definite clue concerning the form of the phase function, and, while we have found no inconsistency with Lambert's function, it is true that other phase functions would have given equally satisfactory results. Our preference for large particles rests, as before, merely upon the evidence from the colors and from the degree of polarization. It is difficult to state the lower limit for the size of the particles consistent with these observations. Obviously, the particles cannot be very large since otherwise the mass of the nebula would be excessive. If we assume that the radius of an average particle

$$\rho = 10\lambda = 5 \times 10^{-4} \text{ cm},$$

we find from Russell's formula

$$\Delta m = 0.8 \frac{hd}{\rho g},$$

where d is the density of the medium and g is the specific weight of the particle, that the total mass of the nebula, for $\Delta m = 6$ mag., is

$$\text{Area of nebula in cm}^2 \times hd \approx 10^3.$$

It is obvious that this mass is not excessive and that even particles having diameters of the order of 0.1 mm would give a mass that would not produce excessive velocities in the stars in its vicinity.

Professor B. Strömgren has pointed out to me that it would be interesting to investigate the possibility of the existence of small particles which absorb light but only scatter a very small amount of it. Such small particles may consist of metals which dissipate a large fraction of the incident energy in the Ohmic currents generated by the electric field of the radiation. By itself, the small amount of observed polarization in reflection nebulae does not preclude this possibility since these small particles would govern the properties of the scattered light only to a slight extent, the larger particles being the

most important sources of the nebular radiation. It is through their absorbing power, which may be selective, that such particles should reveal their presence. The coexistence of selective absorption in CD-24°12684 and its nebula with a large value of the photographic absorption, on the one hand; the absence of strong selective effects in the reflected light of nebulae associated with unobscured stars, and the weakness of the polarization, on the other hand—all support the hypothesis that we are dealing with an agglomeration of large and small particles, both absorbing light but only the larger ones scattering it.

I wish to record my sincere appreciation to Professor Strömgren for his valuable criticism of the work, to Professor Kuiper for his various suggestions concerning the foregoing presentation, to Miss Annie J. Cannon for her kind re-examination of various spectra, and in particular to Professor Struve for his willing and generous co-operation during every phase of the work and for the inspiration which he has provided.

YERKES OBSERVATORY
December 1936

NOTES

A NEW BRIGHT Be STAR¹

Spectrograms of ϵ Orionis recently secured at the Perkins Observatory with the Yerkes auto-collimating spectrograph attached to the 69-inch reflector show that $H\alpha$ occurs in emission in this star. A spectrogram taken on October 19, 1936, indicated that such was the case, but this plate was of poor quality. On January 28, 1937, a good spectrum was secured on a III F plate, and on it the emission component of $H\alpha$ was definitely revealed. ϵ Orionis is not included in Merrill's catalogue² of Be stars, nor is it mentioned as an emission star in any subsequent paper that has come to the attention of the writer. In fact, it will be recalled that the spectrum of ϵ Orionis is often reproduced as a typical example of the Bo spectrum.

The structure of $H\alpha$ in ϵ Orionis is peculiar. The absorption is weak, and it covers an interval of 8.3 angstroms. The emission is not strong, but it is considerably brighter than the continuous background in the neighborhood. The emission component is 3.8 angstroms wide, and it falls on the long wave-length half of the absorption line. On January 28 the absorption and emission velocities of $H\alpha$ were +7 and +45 km/sec, respectively. The velocity of $H\beta$ was +9 km/sec. The $H\alpha$ emission appears to be single.

Five lines of $He I$ were found in the visual region of the spectrum. They are $\lambda\lambda$ 4922, 5016, 5048, 5876, and 6678. Their mean velocity on January 28 was +9 km/sec. The $Na D$ lines are strong, but their velocity of -20 km/sec differs greatly from that of other lines. Two weak lines were found at λ 5412 and λ 5593. The first is tentatively attributed to $He II$ with a velocity of +35 km/sec. The best identification of the second seems to be with $O III$, giving a velocity of

¹ In a letter received after this paper had been sent for publication, Dr. P. W. Merrill states that bright $H\alpha$ in ϵ Orionis has been under observation at Mount Wilson since February 15, 1935. No announcement of these observations has been made.

² *Ap. J.*, 78, 87, 1933; *Mt. W. Contr.*, No. 471.

+19 km/sec. However, these two lines would require excitation to the extent of 78 and 84 volts, respectively.

The great differences in the velocity obtained for absorption lines other than those due to neutral helium and hydrogen are embarrassing, and observations will be continued in order that these discrepancies may be smoothed out or definitely confirmed. Since a difference of 38 km/sec was found between the absorption and emission portions of $H\alpha$, it may be possible that some velocity differences actually exist among absorbing atoms of different elements. The spectrogram of October 19, 1936, shows the emission component of $H\alpha$ displaced toward the red with respect to the $H\alpha$ absorption even farther than it was on January 28, 1937. ϵ Orionis was announced by Frost as a star of variable velocity, but the extensive observations at Lick and Michigan observatories failed to confirm the variability.³ In this respect the case may be similar to that of γ Cassiopeiae.

ERNEST CHERRINGTON, JR.

PERKINS OBSERVATORY
DELAWARE, OHIO
January 30, 1937

³ J. H. Moore, *Pub. Lick Obs.*, 18, 203, 1932.

REVIEWS

Theoretical Astrophysics. By S. ROSSELAND. ("International Series of Monographs on Physics.") Oxford: Clarendon Press, 1936. Pp. xix+355. \$8.00.

So much important astrophysical work has been done within the last few years that a comprehensive discussion of principles and results has become increasingly desirable not only for the new student but no less for the experienced worker who may desire to refresh or extend his knowledge of some less familiar portion of this wide field.

The subject has indeed grown too large to be covered by a single volume, and Professor Rosseland, in the present work, has wisely attempted only "to build up the theory of stellar spectroscopy in a systematic way from the elementary principles of quantum mechanics, ready for the interpretation of astrophysical facts." Within this range he has given us a comprehensive discussion of everything which lies no deeper within the stars than our vision can penetrate—leaving, it is to be hoped, the problems of internal constitution for future consideration. An Introduction, equally admirable for its broad scientific outlook and its literary quality, sketches the historic development from the beginnings of the quantum theory to the present. Then the reader's real work begins with three chapters on "Analytical Dynamics," "Statistical Mechanics," and "Quantum Mechanics." No one could be expected to give a self-contained account of so great a part of modern physics in thirty pages. The student who is already familiar with the rudiments of the subject will find his memory refreshed at the most salient points, while the novice will welcome the references to more detailed presentations of the subject.

Upon this foundation are built more detailed solutions of special problems, leading up to that of the "alkali"-like spectra produced by atoms having one electron outside an electronic core. Criticism of this portion of the book by the present reviewer would be out of place, except to say that there are probably others also who would have found it much easier reading if it had been less compressed.

Chapter vi, on "The Periodic System," gives a lucid account of the influence of Pauli's exclusion principle in producing recurrent regularities in the outer structure of atoms, and of the effects of electronic screening

upon the energy of binding. The latter is presented in the older terminology of shells of electrons running in a field of force—with great gain in intelligibility. The remark that the “additional” electron in *La* is normally bound in a *5p* state is obviously a misprint for *5d*; but the statement that in scandium “all three outer electrons have settled down in *3d* states” is an error—the more surprising because Table 15, at the end of the book, states correctly that two *4s* electrons are present. The discussion of the theory of multiplets, in the following chapter, is again greatly abbreviated. The alternation and displacement laws are clearly stated, though the table of multiplets observed in spark spectra (p. 73) omits a good deal of information contained in the standard work of Bacher and Goudsmit.

The section on “displaced terms” would lead the reader to suppose that they occurred only when two electrons were simultaneously excited—disregarding the very numerous cases in which the limit term in the next highest state of ionization is a metastable term arising from the same electron configuration as the ground state. It is correctly stated that the simultaneous jumping of two electrons produces lines of high frequency; but no reference is made to the transitions between states obtained by adding two different electrons, say *4p* and *4s*, to the same limit term. These lines are often among the strongest in the whole spectrum, and may be of longer wave-length than those arising from similar transitions based on the ground state of the ion, as happens in the alkaline earths.

It may be remarked in passing that the usual system of multiplet nomenclature was not “proposed by Russell and Saunders” but by a committee of the American Physical Society, who, by extensive correspondence and the cordial co-operation of colleagues in many countries, made sure before its publication that the scheme was already accepted by all active workers in the field.

In the discussion of the theory of absorption and emission, the quantum mechanics reappears in full rigor—as it must, since dispersion and the intrinsic width of lines are fully discussed—leading up to the curve of growth. A certain detachment from observation is again present in the statement (p. 104) that “narrow lines, which show this effect of Doppler broadening, will rather tend to be independent of density and optical path.” The case corresponding to the initial steep portion of the curve is dismissed as “too difficult to realize experimentally to be of much value”—though this has recently been utilized, in laboratory absorption measures, to solve the difficult problem of obtaining true relative intensities (*f*-values) for the strongest multiplets of iron.

The discussion of astrophysical problems begins with the transfer of radiation within a star. The problem of determining temperature from the continuous background is described as "one of the most difficult in astrophysics, both observationally and theoretically." The selective absorption, which combines with scattering in the production of the Fraunhofer lines, is attributed mainly to cyclical transitions between atomic states, in which the principle of detailed balancing is not effective. Collisions are dismissed as too infrequent. To the same influence is attributed the main part of the central intensity of the lines. Several recent attempts to devise a second approximation in the theory of line profiles are discussed. The theory of total intensities, which is in a more satisfactory state, and the resulting curve of growth, are clearly discussed. The large excess of the damping constants derived from these curves above the classical values is left unexplained pending "actual calculation of the damping constants from the quantum theory."

The general opacity of stellar atmospheres is attributed mainly to absorption beyond the series limits of excited atoms. The absence of perceptible breaks in the intensity of the continuous spectrum at the known limits (except in the case of hydrogen) is described but not explained.

The effect of stellar rotation on line profiles is next considered—the discussion, as in many other places, being composed largely of summaries of the work of recent investigators. The Zeeman effect in sun-spots is discussed in a few lines, leaving the origin of the fields "an open question" to be explained somehow by the internal motions of the spots. More space is devoted to the general magnetic field of the sun, and an argument is given to show that its intensity is three times as great as the accepted value computed as for an elementary magnet.

The presence of molecular compounds in the stars is discussed at length, and a good deal of space is given to the determination of temperature from band intensities, though the results are admitted to be rough. The dissociation of such compounds is then discussed, with applications to the K-M and R-N sequences and with a brief descriptive summary of planetary atmospheres. The sun's extensive envelopes—chromosphere and corona—are tentatively treated "as dynamic phenomena, the theory of which must be based on considerations of the expansive motion of matter moving away from the sun," and the influences of radiation pressure, corpuscular emission, and magnetic fields are considered. This leads up to the more extensive envelopes which presumably occur in bright-line stars, Wolf-Rayet stars, and novae.

A clear description of forbidden lines and their appearance in nebulae and novae is followed by a rather full discussion of the processes of excita-

tion. Bowen's conclusions as to the mechanism of excitation of the forbidden and permitted lines of oxygen and nitrogen are fully accepted. In the discussion of the latter it is remarked that atoms of these elements cannot get from the ground state to one of the metastable upper states of the forbidden lines without either becoming further ionized or performing a forbidden transition. In the strict sense of the term this is incorrect, for an intersystem transition (triplet-singlet in $O\text{ III}$) would permit the atom to reach the metastable state without ionization. Such transitions are improbable in light atoms—indeed, very few of them have been observed—but they involve dipole radiation and are therefore not “forbidden” in the usual sense. The same rather unconventional use of this word explains the reference in the introduction to the bands of CO_2 in Venus, and CH_4 in Jupiter as “forbidden,” though on pages 259–260 they are described as “higher harmonics.” The telluric oxygen bands, which are described as “forbidden” in the next sentence, are so in the strict sense. A brief discussion of interstellar lines concludes the volume.

The general effect produced by the book—upon one reader, at least—is that it has been compiled from lecture notes of courses which must have been most stimulating. It lacks that close-knit and self-contained character which makes *The Internal Constitution of the Stars* so easy to read, considering the nature of its subject. But it is a valuable book. The occasional lapses, to which perhaps disproportionate attention has here been given, are no more than are useful to keep the student's attention alert.

The English is admirable, with a few distinctive turns of phrase, and the typography and presswork are up to the standard of the Oxford University Press, though the number of misprints is considerable..

H. N. RUSSELL

Princeton University

ERRATA

Volume 85, No. 1, January, 1937, article on “The Absolute Magnitudes of the Stars of Large Proper Motion,” by A. van Maanen:

Page 26, in the Abstract, seventh line, *for* 1 star per 0.2 cubic parsec *read* 0.2 star per cubic parsec.

Page 37, seventh line from bottom, *for* 1 star per 0.204 cubic parsec *read* 0.204 star per cubic parsec.

Page 37, fourth line from bottom, *for* 1 star per 0.196 cubic parsec *read* 0.196 star per cubic parsec.